



MPI-Ph/93-20

May 1993

**Electroweak 1-loop contributions to
top pair production in hadron colliders**

W. BEENAKKER^a, A. DENNER^b, W. HOLLIK^{c,d}, R. MERTIG^e,
T. SACK^{d,f}, D. WACKEROTH^d

^a*DESY, Hamburg (Fed. Rep. Germany)*

^b*CERN-Theory Division, Geneva (Switzerland)*

^c*Fakultät für Physik, Universität Bielefeld,
Bielefeld (Fed. Rep. Germany)*

^d*Max-Planck-Institut für Physik, Werner-Heisenberg-Institut,
Munich (Fed. Rep. Germany)*

^e*Instituut-Lorentz, University of Leiden, Leiden (The Netherlands)*

^f*now at Siemens AG, Munich (Fed. Rep. Germany)*

ABSTRACT

We give a detailed presentation of the electroweak 1-loop contributions to the production mechanisms of top quark pairs, $q\bar{q} \rightarrow t\bar{t}$ and $gg \rightarrow t\bar{t}$, for the energy range of future hadron colliders. The full gauge invariant set of loop diagrams with Higgs, Z^0 , and W^\pm bosons is considered including strong Yukawa couplings. The parton cross sections get sizeable modifications up to 40% and are sensitive to the Higgs boson mass and the Yukawa coupling. Results are also given for the observable hadronic cross section $pp \rightarrow t\bar{t}X$, where the large corrections at the parton level are substantially reduced to the order of a few per cent. For the electroweak Standard Model the maximum contribution is about 7% for a light Higgs boson with $M_\eta = 60$ GeV. For Higgs bosons with $M_\eta > 200$ GeV, the electroweak contributions are typically 2 – 3%.

1 Introduction

The search for the top quark is one of the central tasks of present and future particle physics. The present lower bounds of 103 GeV (D0) and 108 GeV (CDF) for the standard model top mass from direct searches at the Tevatron [1] leave practically no window for the production of $t\bar{t}$ pairs at LEP 200. Presumably proton (anti-)proton colliders will be the only machines for producing top quarks within the next decade. An indirect upper limit for the top quark mass follows from radiative corrections to electroweak precision observables. It is around 200 GeV if the Minimal Standard Model (MSM) is assumed [2]. The lower mass range can be covered by the Tevatron. For large top quark masses, however, proton-proton colliders like LHC and SSC would be required. Moreover only high energy colliders can produce a sufficiently large number of top quarks for a precise determination of its mass and decay properties.

The main production mechanism of top quarks in pp -collisions are described in terms of the parton subprocesses of gluon-gluon fusion and quark-antiquark annihilation. In lowest order these processes are of $\mathcal{O}(\alpha_s^2)$ in the strong coupling constant α_s and they were calculated in [3]. The lowest order electroweak contributions of $\mathcal{O}(\alpha^2)$ to the Drell-Yan annihilation process via γ - and Z -exchange would only be of significance for $m_t < M_Z/2$ [4], which is experimentally ruled out.

Since the $t\bar{t}$ -production cross section in pure QCD contains besides α_s the top quark mass m_t as the only free parameter, it is suitable for a measurement of m_t . For this purpose, higher order contributions have to be taken into account.

Cross sections and distributions including QCD corrections to $\mathcal{O}(\alpha_s^3)$ have been given in [5], and higher order QCD effects close to the production threshold are discussed in [6]. Since the tree level $\mathcal{O}(\alpha^2)$ γ - and Z -exchange diagrams contribute less than 1% at the parton level, they are negligible. On the other hand, electroweak 1-loop contributions of $\mathcal{O}(\alpha\alpha_s^2)$ to the basic QCD processes deserve some closer inspection. They can become important for the energy range of future hadron colliders for two reasons: the large q^2 ($= \hat{s}$ in the parton frame) and the large Yukawa couplings of the (virtual) Higgs bosons to a heavy top quark. Through the virtual presence of the Higgs boson, the $t\bar{t}$ -production becomes model dependent, in particular dependent on the mass of the Higgs boson M_H . From investigations of the $e^+e^- \rightarrow t\bar{t}$ production cross section [7] it is known that the Higgs effects increase $\propto m_t^3$ close to the threshold and modify the cross section significantly, depending crucially on M_H .

In this paper we study the 1-loop contributions from the electroweak interaction to the basic processes $q\bar{q} \rightarrow t\bar{t}$ and $gg \rightarrow t\bar{t}$, and discuss the implications for the observable hadronic cross section $pp \rightarrow t\bar{t}X$. Our main interest is the influence of large Yukawa couplings (and thus the M_H -dependence) on the cross section. For reasons of gauge invariance, the full set of massive gauge boson, Higgs and would-be Goldstone boson exchange diagrams has to be considered. This set of diagrams is UV-finite without renormalisation of the strong coupling constant. Out of the parameters, only mass renormalisation for the top quark in the $t(u)$ -channel top propagators in $gg \rightarrow t\bar{t}$ is required. This is different for pure electroweak processes, which are not UV-finite without coupling constant renormalisation. The IR singular photonic corrections form a separate gauge invariant subset and are not considered here.

The paper is organised as follows:

In section 2 we recall the Born parton cross section of the two top pair production mechanisms and describe their convolution with the parton structure functions in order to obtain the

hadronic cross section. This is followed by a detailed investigation of the electroweak 1-loop contributions to the lowest order matrix element. The compact representation of the $q\bar{q} \rightarrow t\bar{t}$ and $gg \rightarrow t\bar{t}$ cross sections and the discussion of their dependence on the top quark mass and Higgs boson mass close section 3. Finally, in section 4 we present the results for the observable hadronic cross section $pp \rightarrow t\bar{t}X$ and investigate its sensitivity to a variation of the Higgs boson mass between 60 GeV and 1000 GeV. The explicit expressions for the 1-loop corrections and some details of the calculation are summarised in the appendices.

Born parton cross section for $q\bar{q} \rightarrow t\bar{t}$

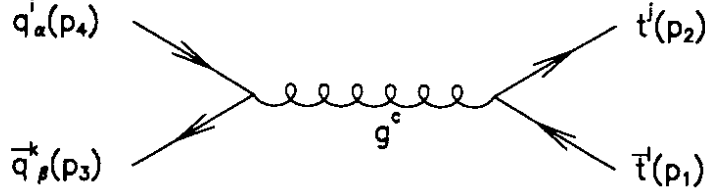


Figure 1: Lowest order Feynman diagram for $q\bar{q} \rightarrow t\bar{t}$

With the QCD Feynman rule from Eq. (2.4) and the momentum assignments of Fig. 1 the leading-order QCD matrix element of $q\bar{q}$ -annihilation is given by:

$$\mathcal{M}_B^{q\bar{q}} = \delta_{\alpha\beta} \bar{u}_t^j(p_2, s_2) (-ig_s T_{jl}^c \gamma_\mu) v_t^l(p_1, s_1) \left(\frac{-ig^{\mu\nu}}{\hat{s}} \right) \times \bar{v}_\beta^k(p_3, s_3) (-ig_s T_{ik}^c \gamma_\nu) u_\alpha^i(p_4, s_4), \quad (2.6)$$

where α, β and $i, j, k, l; c$ are flavour and colour indices, respectively. Straightforward calculation of the square of this Born matrix element $\mathcal{M}_B^{q\bar{q}}$ averaged over the initial spin and colour degrees of freedom and summed over the final ones leads to:

$$\overline{\sum} |\mathcal{M}_B^{q\bar{q}}|^2 = \frac{64\pi^2 \alpha_s^2}{\hat{s}^2} \left\langle \frac{2}{9} \right\rangle \left[\hat{t}^2 + (\hat{s} - 2m_t^2) \hat{t} + \frac{\hat{s}^2}{2} + m_t^4 \right], \quad (2.7)$$

where angular brackets denote the factor due to the summation (average) over the colour degrees of freedom. Integrating the differential cross section between the kinematical limits:

$$m_t^2 - \frac{1}{2}\hat{s} - \frac{1}{2}\hat{s}\sqrt{1 - \frac{4m_t^2}{\hat{s}}} \leq \hat{t} \leq m_t^2 - \frac{1}{2}\hat{s} + \frac{1}{2}\hat{s}\sqrt{1 - \frac{4m_t^2}{\hat{s}}} \quad (2.8)$$

yields the total $q\bar{q} \rightarrow t\bar{t}$ cross section as given in [3]:

$$\hat{\sigma}_B^{q\bar{q}}(\hat{s}) = \frac{4\pi\alpha_s^2}{3} \left\langle \frac{2}{9} \right\rangle \frac{1}{\hat{s}^2} \sqrt{1 - \frac{4m_t^2}{\hat{s}}} (\hat{s} + 2m_t^2). \quad (2.9)$$

Born parton cross section for $gg \rightarrow t\bar{t}$

The gluon fusion matrix element is composed of the three different production channels (s -, t -, u -channel) as follows [3]:

$$\mathcal{M}_B^{gg} = g_s^2 \epsilon_4^\mu(p_4) \epsilon_3^\nu(p_3) \bar{u}_t^j(p_2, s_2) T_{\mu\nu}^{ab} v_t^l(p_1, s_1), \quad (2.10)$$

where

$$\begin{aligned} T_{\mu\nu}^{ab} = & \frac{T_{jl}^c f_{abc}}{\hat{s}} [(\not{p}_4 - \not{p}_3)g_{\mu\nu} + (2p_3 + p_4)_\mu \gamma_\nu - (2p_4 + p_3)_\nu \gamma_\mu] \quad : s\text{-channel} \\ & + \frac{(-i)T_{jm}^a T_{ml}^b}{\hat{t} - m_t^2} \gamma_\mu (\not{p}_3 - \not{p}_1 + m_t) \gamma_\nu \quad : t\text{-channel} \\ & + \frac{(-i)T_{jm}^b T_{ml}^a}{\hat{u} - m_t^2} \gamma_\nu (\not{p}_4 - \not{p}_1 + m_t) \gamma_\mu \quad : u\text{-channel}. \end{aligned} \quad (2.11)$$

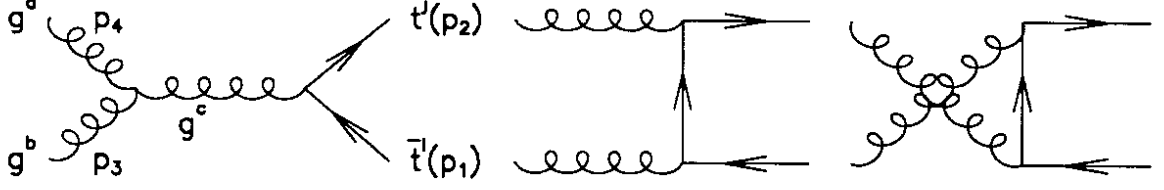


Figure 2: Lowest order Feynman diagrams for $gg \rightarrow t\bar{t}$

Since the initial state gluons are unpolarised the computation of $\overline{\sum} | \mathcal{M}_B^{gg} |^2$ requires an averaging over the polarisation states of the initial gluons. The polarisation sum of the gluon polarisation vectors $\epsilon_4^\mu(\lambda_4, p_4)$ and $\epsilon_3^\nu(\lambda_3, p_3)$ has to be chosen in such a way that only the physical (transverse) polarisation states remain and the unphysical one (longitudinal) does not contribute to the matrix element:

$$\sum_{\lambda=1,2} \epsilon_\mu^*(\lambda, k) \epsilon_\nu(\lambda, k) = -g_{\mu\nu} + Q_{\mu\nu}$$

$$Q_{\mu\nu} = \frac{k_\mu \eta_\nu + k_\nu \eta_\mu}{\eta k} - \frac{\eta^2 k_\mu k_\nu}{(k\eta)^2}, \quad (2.12)$$

where η fulfills the conditions $k\eta \neq 0$ and $\eta\epsilon = 0$. The vector η has been chosen to be the sum of the gluon four vectors p_3, p_4 , so that $Q_{\mu\nu}$ is given by:

$$Q_{\mu\nu} = 2 \frac{p_{3\mu} p_{4\nu} + p_{3\nu} p_{4\mu}}{\hat{s}}. \quad (2.13)$$

Eqs. (2.3), (2.10) completely determine the differential $gg \rightarrow t\bar{t}$ cross section at parton level, which can be written as follows [3]:

$$\frac{d\hat{\sigma}_B^{gg}}{d\hat{t}} = \frac{\pi\alpha_s^2}{64\hat{s}^2} \left[\langle 12 \rangle M_{ss} + \langle \frac{16}{3} \rangle M_{tt} + \langle \frac{16}{3} \rangle M_{uu} + \langle 6 \rangle M_{st} + \langle 6 \rangle M_{su} + \langle -\frac{2}{3} \rangle M_{tu} \right], \quad (2.14)$$

with

$$\begin{aligned} M_{ss} &= \frac{4}{\hat{s}^2} (\hat{t} - m_t^2)(\hat{u} - m_t^2) : | \text{s-channel} |^2 \\ M_{tt} &= \frac{2}{(\hat{t} - m_t^2)^2} \{ (\hat{t} - m_t^2)(\hat{u} - m_t^2) - 2m_t^2(\hat{t} - m_t^2) - 4m_t^4 \} : | \text{t-channel} |^2 \\ M_{uu} &= \frac{2}{(\hat{u} - m_t^2)^2} \{ (\hat{t} - m_t^2)(\hat{u} - m_t^2) - 2m_t^2(\hat{u} - m_t^2) - 4m_t^4 \} : | \text{u-channel} |^2 \\ M_{st} &= \frac{4}{\hat{s}(\hat{t} - m_t^2)} \{ m_t^4 - \hat{t}(\hat{s} + \hat{t}) \} : 2(\text{s-channel})(\text{t-channel})^* \\ M_{su} &= \frac{4}{\hat{s}(\hat{u} - m_t^2)} \{ m_t^4 - \hat{u}(\hat{s} + \hat{u}) \} : 2(\text{s-channel})(\text{u-channel})^* \\ M_{tu} &= \frac{4m_t^2}{(\hat{t} - m_t^2)(\hat{u} - m_t^2)} \{ \hat{s} - 4m_t^2 \} : 2(\text{t-channel})(\text{u-channel})^*. \end{aligned} \quad (2.15)$$

After carrying out the \hat{t} -integration the total Born parton cross section for the gluon fusion is given by:

$$\hat{\sigma}_B^{gg}(\hat{s}) = \frac{\pi\alpha_s^2}{64\hat{s}} \left(\langle 12 \rangle \frac{1}{3} (2 + \rho)\beta + \langle \frac{16}{3} \rangle \{ (4 + 2\rho) \ln \frac{1 + \beta}{1 - \beta} - 4(1 + \rho)\beta \} \right)$$

$$+ \langle 6 \rangle \left\{ 2\rho \ln \frac{1+\beta}{1-\beta} - 4(1+\rho)\beta \right\} + \left\langle -\frac{2}{3} \right\rangle 2\rho(1-\rho) \ln \frac{1+\beta}{1-\beta} \right), \quad (2.16)$$

where $\beta = \sqrt{1-\rho}$ and $\rho = \frac{4m_t^2}{s}$.

The hadronic cross section for $pp \rightarrow t\bar{t}X$

The hadronic cross section is composed of the perturbatively calculable short distance parton cross section $\hat{\sigma}$ and the universal, scale dependent QCD parton distribution functions $f_i(x_1, Q)$, $f_j(x_2, Q)$. For protons carrying the momentum P_1 or P_2 with the center-of-mass energy $S = (P_1 + P_2)^2$ the hadronic cross section is given by [8]:

$$\sigma(P_1, P_2) = \sum_{i,j} \int dx_1 dx_2 f_i(x_1, Q) f_j(x_2, Q) \hat{\sigma}_{ij}(p_1, p_2, \alpha_s(\mu)), \quad (2.17)$$

where the sum runs over all incoming partons carrying a fraction of the proton momenta ($p_{1,2} = x_{1,2}P_{1,2}$). Since the factorisation scale Q and the renormalisation scale μ have to be of the same order of magnitude we do not distinguish the two and conventionally take both as the top quark mass: $Q = \mu = m_t$. With the parton luminosity [9]:

$$\frac{dL_{ij}}{d\tau} = \frac{1}{1+\delta_{ij}} \int_{\tau_0}^1 \frac{dx_1}{x_1} \left[f_i(x_1, \mu) f_j\left(\frac{\tau}{x_1}, \mu\right) + (1 \leftrightarrow 2) \right], \quad (2.18)$$

where $\tau_0 = \frac{4m_t^2}{S}$, the resulting hadronic cross section can be written as:

$$\sigma(S) = \sum_{i,j} \int_{\tau_0}^1 \frac{d\tau}{\tau} \left(\frac{1}{S} \frac{dL_{ij}}{d\tau} \right) (\hat{\sigma}_{ij}). \quad (2.19)$$

In order to derive the $pp \rightarrow t\bar{t}$ cross section in leading order QCD the parton cross sections of the dominant production mechanisms, gluon fusion and $q\bar{q}$ -annihilation, calculated in the previous sections, have to be convoluted with the quark or gluon distribution functions. The application of Eq. (2.19) yields the following hadronic cross section:

$$\sigma_B(S) = \int_{\tau_0}^1 \frac{d\tau}{\tau} \left(\frac{1}{S} \frac{dL_{q\bar{q}}}{d\tau} \hat{\sigma}_B^{q\bar{q}}(\hat{s}) + \frac{1}{S} \frac{dL_{gg}}{d\tau} \hat{\sigma}_B^{gg}(\hat{s}) \right). \quad (2.20)$$

For the explicit numerical calculation we used the parton distribution functions obtained by including the muon data of the BCDMS collaboration as it is described in [10].

3 Electroweak radiative corrections to the parton cross section

3.1 Structure of 1-loop contributions

We examine the $\mathcal{O}(\alpha\alpha_s^2)$ electroweak contributions to both the $q\bar{q} \rightarrow t\bar{t}$ and $gg \rightarrow t\bar{t}$ subprocesses. The loop diagrams under consideration are shown schematically in Figs. 3, 4. The complete set is gauge invariant, IR finite, and also UV finite even without renormalisation of the strong coupling constant (only mass renormalisation in the $t(u)$ -channel is required together with external wave function renormalisation of the fermions).

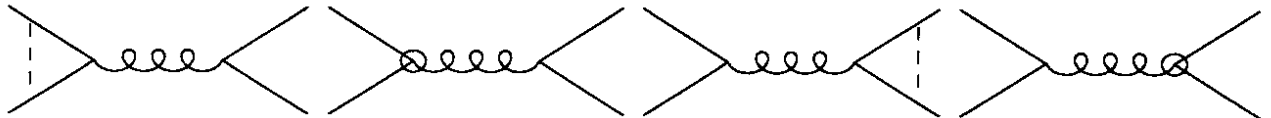


Figure 3: Electroweak $\mathcal{O}(\alpha\alpha_s^2)$ contributions to the $q\bar{q}$ -annihilation (dashed lines denote Z^0 , W^\pm and Higgs bosons, diagrams with ringed vertices and lines denote the counter terms)

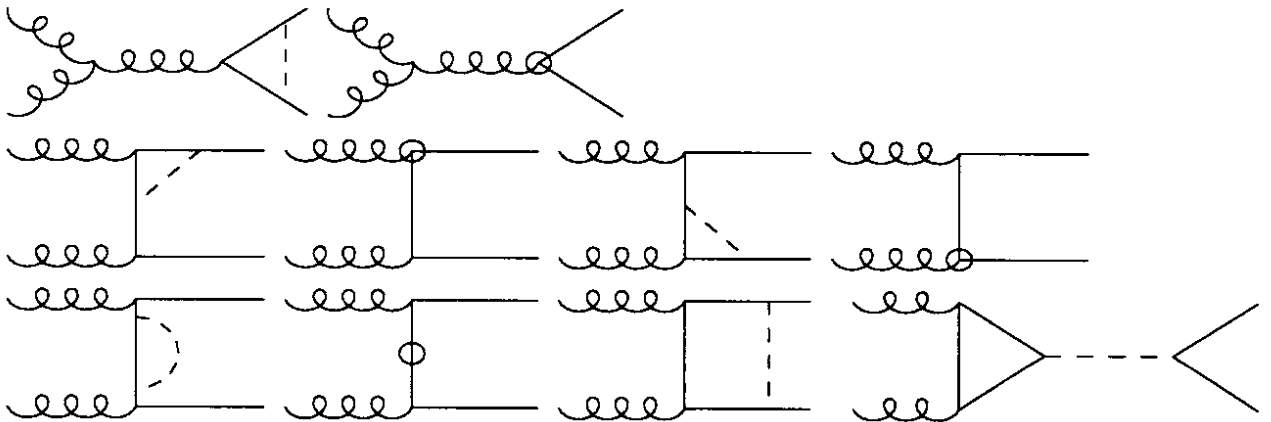


Figure 4: Electroweak $\mathcal{O}(\alpha\alpha_s^2)$ contributions to the gluon fusion (u -channel diagrams are not explicitly shown)

The 1-loop expansion of the $q\bar{q}$ -annihilation and gluon fusion amplitudes consists of the genuine 1-loop diagrams and the tree diagrams involving the counter terms for the $gq\bar{q}$ -vertex and the top quark propagator. The counter terms are formally obtained by the transformation for the left-and right handed quark fields and for the top quark mass

$$\Psi_{L,R} \rightarrow \sqrt{Z_{L,R}} \Psi_{L,R} \ , \ m_t \rightarrow m_t - \delta m_t$$

where

$$\Psi_{L,R} = \frac{1 \mp \gamma_5}{2} \Psi \ , \ Z_{L,R} = 1 + \delta Z_{L,R}$$

in the Lagrangian, which describes the free propagation of the top quark and its interaction with the gluon field G_a^μ :

$$\mathcal{L} = \bar{\Psi}(\not{p} - m_t)\Psi + \bar{\Psi}(-g_s T^a)\gamma_\mu \Psi G_a^\mu \ .$$

This yields the counter terms for the gluon-top quark vertex and the top quark self energy as follows:

$$\begin{array}{c} \text{g}^c \end{array} \begin{array}{c} \text{t} \\ \text{t} \end{array} \quad : \quad i\delta\Lambda_\mu = -ig_s T^c \gamma_\mu (\delta Z_V - \delta Z_A \gamma_5) \quad (3.1)$$

$$\begin{array}{c} \text{t}(p) \end{array} \quad : \quad i\delta\Sigma = i [\not{p} (\delta Z_V - \delta Z_A \gamma_5) - m_t \delta Z_V + \delta m_t] , \quad (3.2)$$

where

$$\delta Z_{V,A} = \frac{1}{2} (\delta Z_L \pm \delta Z_R) . \quad (3.3)$$

The finite parts of the counter terms are fixed by the following renormalisation conditions (the symbol $\hat{}$ denotes renormalised quantities):

- The pole of the top quark propagator defines the on-shell top quark mass:

$$\hat{\Sigma}(\not{p} = m_t) = 0 , \quad (3.4)$$

fixing the mass renormalisation constant as follows:

$$\frac{\delta m_t}{m_t} = (-\Sigma_V - \Sigma_S)|_{p^2=m_t^2} . \quad (3.5)$$

- The residue of the fermion propagator is equal to one, equivalent to:

$$\lim_{\not{p} \rightarrow m} \frac{1}{\not{p} - m} \hat{\Sigma}(\not{p}) = 0 , \quad (3.6)$$

fixing the wave function renormalisation constants by:

$$\begin{aligned} \delta Z_V &= -\Sigma_V(p^2 = m_t^2) - 2m_t^2 \frac{\partial}{\partial p^2} (\Sigma_V + \Sigma_S)|_{p^2=m_t^2} \\ \delta Z_A &= -\Sigma_A(p^2 = m_t^2) . \end{aligned} \quad (3.7)$$

Thus, the counter terms according to Eqs. (3.1), (3.2) are expressed by the top quark self energy (and its derivative), which has been decomposed as follows:

$$\Sigma(\not{p}) = \not{p} (\Sigma_V(p^2) - \Sigma_A(p^2) \gamma_5) + m_t \Sigma_S(p^2) \quad (3.8)$$

with scalar functions $\Sigma_{V,A,S}$. These operations lead to finite vertex corrections $\hat{\Lambda}_\mu$ and self energies $\hat{\Sigma}$, which consist of the sum of the 1-loop diagrams Λ_μ , Σ and their counter terms $\delta\Lambda_\mu$, $\delta\Sigma$:

$$\begin{array}{c} \text{gluon vertex} \end{array} + \begin{array}{c} \text{ghost vertex} \end{array} \quad : \quad i\hat{\Lambda}_\mu = i\Lambda_\mu + i\delta\Lambda_\mu \quad (3.9)$$

$$\begin{array}{c} \text{self energy} \end{array} + \begin{array}{c} \text{counter term} \end{array} \quad : \quad i\hat{\Sigma} = i\Sigma + i\delta\Sigma . \quad (3.10)$$

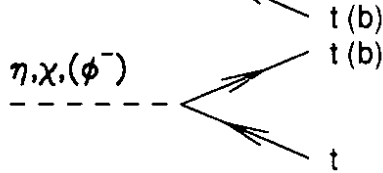
The finite initial state qqg -vertices are obtained analogously by substituting $m_t \rightarrow m_q$.

3.2 Structure of amplitudes for $pp \rightarrow t\bar{t}$ subprocesses

Within the Minimal Standard Model (MSM) the top-gluon vertex and the top quark self energy are modified due to the exchange of vector bosons Z^0 , W^\pm and the Higgs boson η , together with the unphysical components χ , Φ in the Feynman-'t Hooft gauge. The Higgs bosons have Yukawa couplings $\propto m_t/M_W$ to the top quark that can be written in the following generalised form ($s_w = \sin \theta_w$, M_W : mass of the charged gauge boson W^\pm):



$$: \frac{ie m_t}{2s_w M_W} (c_s - c_p \gamma_5) \quad (3.11)$$



$$: \frac{ie m_t}{2s_w M_W} (c_s + c'_p \gamma_5) . \quad (3.12)$$

For the quark-gauge boson coupling we use the following representation:



$$: ie \gamma_\mu (g_V - g_A \gamma_5) . \quad (3.13)$$

The coupling constants g_V, g_A, c_s, c_p, c'_p in the Feynman-'t Hooft gauge within the MSM are specified in Tab. 1.

	Z^0	W^\pm	η	χ	Φ^\pm
g_V	$\frac{T_3^f - 2Q_f s_w^2}{2s_w c_w}$	$\frac{1}{2\sqrt{2}s_w}$	-	-	-
g_A	$\frac{T_3^f}{2s_w c_w}$	g_V	-	-	-
c_s	-	-	(-1)	0	$\frac{1}{\sqrt{2}}(1 - \frac{m_b}{m_t})$
c_p	-	-	0	(-i)	$\frac{1}{\sqrt{2}}(1 + \frac{m_b}{m_t})$
c'_p	-	-	0	$-c_p$	c_p

Table 1: Gauge- and Higgs boson couplings to fermions (Q_f, T_3^f : charge and third isospin component of the fermion f , $c_w = \cos \theta_w$, m_b : bottom quark mass)

The differential parton cross section for the $q\bar{q}$ -annihilation ($i = q\bar{q}$) and the gluon fusion ($i = gg$) is obtained from Eq. (2.3) by using the spin and colour averaged transition amplitude squared up to $\mathcal{O}(\alpha_s^2)$:

$$\begin{aligned} \overline{\sum} |\mathcal{M}_i(\hat{s}, \hat{t}, \hat{u})|^2 &= \overline{\sum} |(\mathcal{M}_B^i(\alpha_s) + \delta\mathcal{M}_i(\alpha_s))|^2 \\ &= \overline{\sum} |\mathcal{M}_B^i|^2 + \overline{\sum} 2\text{Re}[\delta\mathcal{M}_i \times \mathcal{M}_B^{i*}] + \mathcal{O}(\alpha_s^2 \alpha_s^2) . \end{aligned} \quad (3.14)$$

The matrix elements $\delta\mathcal{M}_{q\bar{q}, gg}$ comprise the electroweak next-to-leading order contributions to the $(q\bar{q}, gg)$ -subprocesses, which are shown in Figs. 3, 4.

The electroweak 1-loop corrections for $q\bar{q}$ -annihilation originate from the exchange of gauge bosons and Higgs particles in the final as well as the initial state. Due to the mass dependence of the Yukawa coupling ($\propto m_q$, $q = u, d, \dots$) the Higgs contribution to the initial state vertex correction $\hat{\Lambda}_\mu^{s,in}$ is negligible. The correction for the $q\bar{q}$ -subprocess is given by:

$$\delta\mathcal{M}_{q\bar{q}} = \delta\mathcal{M}_{q\bar{q}}^{in} + \delta\mathcal{M}_{q\bar{q}}^{fin}, \quad (3.15)$$

where

$$\begin{aligned} \delta\mathcal{M}_{q\bar{q}}^{in} &= \delta_{\alpha\beta} \bar{u}_t^j(p_2, s_2) (-ig_s T_{jl}^c \gamma_\mu) v_t^l(p_1, s_1) \left(\frac{-ig^{\mu\nu}}{\hat{s}} \right) \times \\ &\quad \bar{v}_\beta^k(p_3, s_3) (i\hat{\Lambda}_\nu^{s,in}) u_\alpha^i(p_4, s_4) \\ \delta\mathcal{M}_{q\bar{q}}^{fin} &= \delta_{\alpha\beta} \bar{u}_t^j(p_2, s_2) (i\hat{\Lambda}_\mu^{s,fin}) v_t^l(p_1, s_1) \left(\frac{-ig^{\mu\nu}}{\hat{s}} \right) \times \\ &\quad \bar{v}_\beta^k(p_3, s_3) (-ig_s T_{ik}^c \gamma_\nu) u_\alpha^i(p_4, s_4). \end{aligned} \quad (3.16)$$

The renormalised quark-gluon vertex can be described as an effective vertex with finite form factors in the following way [$p(\bar{p})$: momentum of the (anti)quark]:

$$i\hat{\Lambda}_\mu^s(\hat{s}) = (-ig_s T^c) \frac{\alpha}{4\pi} [\gamma_\mu F_V + \gamma_\mu \gamma_5 G_A + (\bar{p} - p)_\mu \frac{1}{2m_q} F_M + (\bar{p} + p)_\mu \gamma_5 G_E]. \quad (3.17)$$

Since, as a result of the interference with the Born matrix element, G_A and G_E do not contribute to $\delta\mathcal{M}_{q\bar{q}}$ we need only the form factors F_V and F_M . For the initial state vertex contribution with light quarks also the magnetic term F_M is negligible. Thus the matrix element with initial state corrections is given by:

$$\delta\mathcal{M}_{q\bar{q}}^{in} = \alpha\alpha_s \frac{iT_{ik}^c T_{jl}^c}{\hat{s}} \bar{u}_t^j(p_2, s_2) \gamma_\mu v_t^l(p_1, s_1) \bar{v}_\alpha^k(p_3, s_3) \gamma^\mu u_\alpha^i(p_4, s_4) \sum_{V=Z^0, W^\pm} F_V^G(\hat{s}, m_q, M_V), \quad (3.18)$$

and with final state corrections we get:

$$\delta\mathcal{M}_{q\bar{q}}^{fin} = \alpha\alpha_s \frac{iT_{ik}^c T_{jl}^c}{\hat{s}} \bar{u}_t^j(p_2, s_2) [\gamma_\mu F_V(\hat{s}) + \frac{1}{2m_t} (p_1 - p_2)_\mu F_M(\hat{s})] v_t^l(p_1, s_1) \bar{v}_\alpha^k(p_3, s_3) \gamma^\mu u_\alpha^i(p_4, s_4) \quad (3.19)$$

with

$$F_{V,M}(\hat{s}) = \left(\frac{m_t}{2s_w M_W} \right)^2 \sum_{S=\eta, \chi, \Phi^\pm} F_{V,M}^H(\hat{s}, m_t, M_S) + \sum_{V=Z^0, W^\pm} F_{V,M}^G(\hat{s}, m_t, M_V). \quad (3.20)$$

The form factors $F_{V,M}^{H,G}(\hat{s}, m_q, M_{S,V})$ are listed in App. A.2.

For the sake of cleanness we decompose the correction $\delta\mathcal{M}_{gg}$ to the Born matrix element for the gluon fusion in the following different types of 1-loop diagrams, which are shown in Fig. 4: vertex corrections $\delta\mathcal{M}_{gg}^{Vertex}$, top quark self energies $\delta\mathcal{M}_{gg}^\Sigma$, box diagrams $\delta\mathcal{M}_{gg}^\square$ and fermionic triangle diagrams $\delta\mathcal{M}_{gg}^\triangle$. These contributions can be summarised in terms of coefficients of so

called standard matrix elements $M_i^{(V,A),(t,u)}$, so that we obtain a compact representation of the transition amplitude to $\mathcal{O}(\alpha_s)$:

$$\begin{aligned}\delta\mathcal{M}_{gg} &= \delta\mathcal{M}_{gg}^{Vertex} + \delta\mathcal{M}_{gg}^{\Sigma} + \delta\mathcal{M}_{gg}^{\square} + \delta\mathcal{M}_{gg}^{\triangle} \\ &= \sum_{\substack{i=1,\dots,7; \\ 11,\dots,17}} M_i^{V,(t,u)} (H_i + G_i)^{(s,t,u)}.\end{aligned}\quad (3.21)$$

The matrix elements $M_i^{A,(t,u)}$ (they are $\propto \gamma_5$) do not contribute by interference with \mathcal{M}_B^{gg} . The coefficients H_i, G_i comprise the contributions of all Higgs bosons of the model under consideration (MSM) and of the massive gauge bosons, respectively. The standard matrix elements contain the information about the Dirac matrix structure of the corrections and are given in App. B.1.

The vertex correction $\delta\mathcal{M}_{gg}^{Vertex}$ represents the sum of different production channel (s, t, u) contributions:

$$\delta\mathcal{M}_{gg}^{Vertex} = \delta\mathcal{M}_{gg}^{V,s} + \delta\mathcal{M}_{gg}^{V,t} + \delta\mathcal{M}_{gg}^{V,u}.\quad (3.22)$$

Since the vertex corrections to the $g\bar{t}\bar{t}$ -vertex in the gluon fusion subprocess and the final state contribution $\Lambda_\mu^{s,fin}$ to the $q\bar{q} \rightarrow t\bar{t}$ matrix element of Eq. (3.16) are the same, the matrix element $\delta\mathcal{M}_{gg}^{V,s}$ can be expressed by the form factors F_V, F_M already known from Eq. (3.20):

$$\begin{aligned}\delta\mathcal{M}_{gg}^{V,s} &= \bar{u}_t^j(p_2, s_2) (i\hat{\Lambda}_\mu^{s,fin}) v_t^l(p_1, s_1) \left(\frac{-ig^{\mu\nu}}{\hat{s}} \right) \epsilon_4^\rho(p_4) \epsilon_3^\sigma(p_3) \times \\ &\quad (-g_s f_{abc}) \{ (p_4 - p_3)_\nu g_{\rho\sigma} + (p_4 + 2p_3)_\rho g_{\sigma\nu} - (p_3 + 2p_4)_\sigma g_{\nu\rho} \} \\ &= \frac{\alpha_s}{\hat{s}} T_{jl}^c f_{abc} \left\{ [M_2^{V,t} - 2M_3^{V,t}] F_V(\hat{s}) \right. \\ &\quad \left. + [(\hat{t} - \hat{u}) M_{12}^{V,t} - 4M_{15}^{V,t} + 4M_{17}^{V,t}] \frac{F_M(\hat{s})}{2m_t^2} \right\}.\end{aligned}\quad (3.23)$$

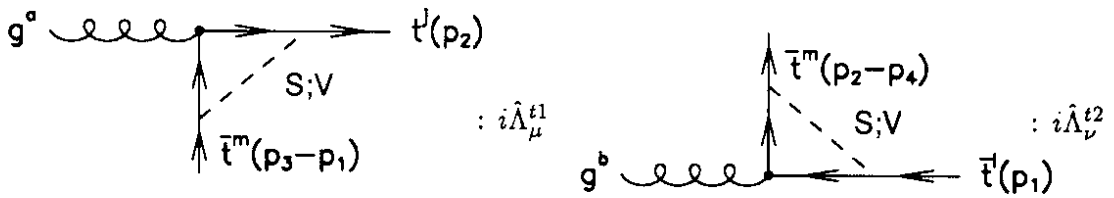


Figure 5: Feynman diagrams for the t -channel vertex corrections

We give explicitly only the results for the t -channel contributions to $\delta\mathcal{M}_{gg}^X$ ($X = Vertex, \Sigma, \square$). The application of the following substitutions to $\delta\mathcal{M}_{gg}^{X,t}$ leads to the corresponding u -channel matrix elements:

$$\hat{t} \leftrightarrow \hat{u}, \quad p_3 \leftrightarrow p_4, \quad \epsilon_3 \leftrightarrow \epsilon_4, \quad T^a \leftrightarrow T^b.\quad (3.24)$$

The 1-loop diagrams shown in Fig. 5 lead to the following t -channel vertex contribution:

$$\begin{aligned}\delta\mathcal{M}_{gg}^{V,t} &= \epsilon_4^\mu(p_4) \epsilon_3^\nu(p_3) \bar{u}_t^j(p_2, s_2) \times \\ &\quad \left\{ \frac{i}{\hat{t} - m_t^2} [(i\hat{\Lambda}_\mu^{t1}) (\not{p}_3 - \not{p}_1 + m_t) (-ig_s T_{ml}^b \gamma_\nu)] \right\}\end{aligned}$$

$$\begin{aligned}
& +(-ig_s T_{jm}^a \gamma_\mu) (\not{p}_2 - \not{p}_4 + m_t) (i \hat{\Lambda}_\nu^{t2}) \} v_t^l(p_1, s_1) \\
= & \frac{\alpha \alpha_s (iT_{jm}^a T_{ml}^b)}{\hat{t} - m_t^2} \sum_{i=1, \dots, 7; 11, \dots, 17} M_i^{V,t} \left[\left(\frac{m_t}{2s_w M_W} \right)^2 \sum_S H_i^{V,t} + \sum_V G_i^{V,t} \right]. \quad (3.25)
\end{aligned}$$

The vertex corrections $\hat{\Lambda}_\mu^{t1}$, $\hat{\Lambda}_\nu^{t2}$ contain the counter terms according to Eq. (3.9).

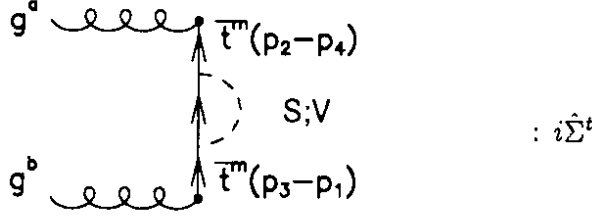


Figure 6: Feynman diagram for the t -channel self energy

The top quark self energy (Fig. 6) contributes to the t - and u -channel matrix element:

$$\delta \mathcal{M}_{gg}^\Sigma = \delta \mathcal{M}_{gg}^{\Sigma,t} + \delta \mathcal{M}_{gg}^{\Sigma,u}, \quad (3.26)$$

where

$$\begin{aligned}
\delta \mathcal{M}_{gg}^{\Sigma,t} &= \epsilon_4^\mu(p_4) \epsilon_3^\nu(p_3) \bar{u}_t^j(p_2, s_2) \times \\
& \frac{g_s^2 T_{jm}^a T_{ml}^b}{(\hat{t} - m_t^2)^2} \gamma_\mu (\not{p}_2 - \not{p}_4 + m_t) (i \hat{\Sigma}^t) (\not{p}_3 - \not{p}_1 + m_t) \gamma_\nu v_t^l(p_1, s_1) \\
&= \frac{\alpha \alpha_s (iT_{jm}^a T_{ml}^b)}{(\hat{t} - m_t^2)^2} \sum_{i=1, \dots, 7; 11, \dots, 17} M_i^{V,t} \left[\left(\frac{m_t}{2s_w M_W} \right)^2 \sum_S H_i^{\Sigma,t} + \sum_V G_i^{\Sigma,t} \right]. \quad (3.27)
\end{aligned}$$

The coefficients $(H, G)_i^{(V,\Sigma),(t,u)}$ are finite and the explicit formulae are given in App. A.3.

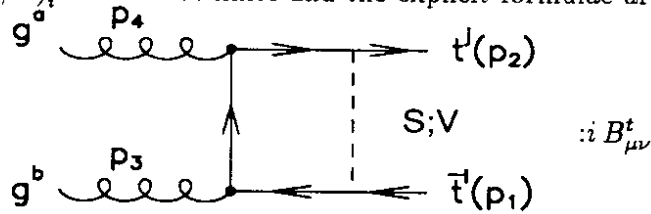


Figure 7: Box diagram

The box diagram $B_{\mu\nu}^t$ of Fig. 7 contains only finite four-point integrals $D_{\mu\nu}$. According to Passarino and Veltman [11] they are expanded in terms of all possible Lorentz covariant combinations of the external momenta (as well as the metric tensor $g_{\mu\nu}$) as it is described in App. C.3. The box matrix element can be written as follows:

$$\delta \mathcal{M}_{gg}^\square = \delta \mathcal{M}_{gg}^{\square,t} + \delta \mathcal{M}_{gg}^{\square,u}, \quad (3.28)$$

where

$$\begin{aligned}
\delta \mathcal{M}_{gg}^{\square,t} &= \epsilon_4^\mu(p_4) \epsilon_3^\nu(p_3) \bar{u}_t^j(p_2, s_2) i B_{\mu\nu}^t v_t^l(p_1, s_1) \\
&= \alpha \alpha_s (iT_{jm}^a T_{ml}^b) \sum_{i=1, \dots, 7; 11, \dots, 17} M_i^{V,t} \left[\left(\frac{m_t}{2s_w M_W} \right)^2 \sum_S H_i^{\square,t} + \sum_V G_i^{\square,t} \right]. \quad (3.29)
\end{aligned}$$

The coefficients $(H, G)_i^{\square, t}$ are given in App. A.3.

Finally we give the matrix element $\delta\mathcal{M}_{gg}^{\square}$ for the $t\bar{t}$ -production via the s -channel-Higgs-exchange of a virtual neutral, scalar Higgs boson η with its width Γ_η .

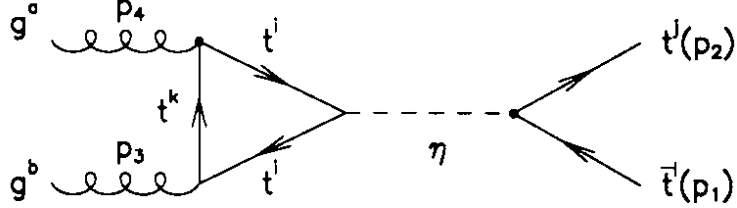


Figure 8: Feynman diagram for the s -channel-Higgs-exchange

The diagram in Fig. 8 and the corresponding crossed one yield $(M_{12}^{V,u} = M_{12}^{V,t})$:

$$\delta\mathcal{M}_{gg}^{\square} = M_{12}^{V,t} \left(\frac{m_t}{2s_w M_W} \right)^2 \frac{(-i \delta^{ab}) \alpha \alpha_s}{(\hat{s} - M_\eta^2)^2 + (M_\eta \Gamma_\eta)^2} H_{12}^{\square}(\hat{s}, M_\eta). \quad (3.30)$$

The previous results allow for the following compact representation of the matrix element to $\mathcal{O}(\alpha_s)$ for the gluon fusion:

$$\begin{aligned} \delta\mathcal{M}_{gg} = & \alpha \alpha_s \left\{ \frac{f_{abc} T_{jl}^c}{\hat{s}} \left[(M_2^{V,t} - 2M_3^{V,t}) F_V(\hat{s}) + ((\hat{t} - \hat{u}) M_{12}^{V,t} \right. \right. \\ & \left. \left. - 4M_{15}^{V,t} + 4M_{17}^{V,t}) \frac{F_M(\hat{s})}{2m_t^2} \right] + \frac{(-i \delta^{ab}) M_{12}^{V,t} \rho_{12}^{\square}(\hat{s}, M_\eta)}{(\hat{s} - M_\eta^2)^2 + (M_\eta \Gamma_\eta)^2} \right. \\ & + \sum_{\substack{i=1, \dots, 7 \\ 11, \dots, 17}} \left(i T_{jm}^a T_{ml}^b M_i^{V,t} \left[\frac{\rho_i^{V,t}(\hat{t})}{\hat{t} - m_t^2} + \frac{\rho_i^{\Sigma,t}(\hat{t})}{(\hat{t} - m_t^2)^2} + \rho_i^{\square,t}(\hat{t}, \hat{s}) \right] \right. \\ & \left. \left. + i T_{jm}^b T_{ml}^a M_i^{V,u} \left[\frac{\rho_i^{V,u}(\hat{u})}{\hat{u} - m_t^2} + \frac{\rho_i^{\Sigma,u}(\hat{u})}{(\hat{u} - m_t^2)^2} + \rho_i^{\square,u}(\hat{u}, \hat{s}) \right] \right) \right\}, \quad (3.31) \end{aligned}$$

where the coefficients ρ_i^{\square} denote the following contributions:

$$\rho_i^{(V,\Sigma,\square),(t,u)} = \left(\frac{m_t}{2s_w M_W} \right)^2 \sum_S H_i^{(V,\Sigma,\square),(t,u)} + \sum_V G_i^{(V,\Sigma,\square),(t,u)} \quad (3.32)$$

$$\rho_{12}^{\square} = \left(\frac{m_t}{2s_w M_W} \right)^2 H_{12}^{\square}. \quad (3.33)$$

The u -channel contributions result from the application of the transformations according to Eq. (3.24) to the t -channel coefficients.

3.3 Parton cross sections

The differential parton cross section to order α_s^2 is completely determined by the results of the last sections up to the remaining contraction of the matrix elements $\delta\mathcal{M}_i$ with the Born matrix element \mathcal{M}_B^i according to Eq. (3.14) ($i = q\bar{q}, gg$):

$$\delta \frac{d\hat{\sigma}_i(\hat{t}, \hat{s})}{d\hat{t}} = \frac{1}{16\pi \hat{s}^2} 2\text{Re} \overline{\sum} [\delta\mathcal{M}_i \times \mathcal{M}_B^{i*}]. \quad (3.34)$$

For the $q\bar{q} \rightarrow t\bar{t}$ process one gets the two contributions:

INITIAL STATE

$$\delta \frac{d\hat{\sigma}_{q\bar{q}}^{in}(\hat{s}, \hat{t})}{d\hat{t}} = \frac{\alpha\alpha_s^2}{\hat{s}^4} \left\langle \frac{2}{9} \right\rangle 2\text{Re} \left[\sum_V F_V^G(\hat{s}, m_q, M_V) \right] (\hat{t}^2 + (\hat{s} - 2m_t^2)\hat{t} + \frac{\hat{s}^2}{2} + m_t^4) \quad (3.35)$$

FINAL STATE

$$\delta \frac{d\hat{\sigma}_{q\bar{q}}^{fin}(\hat{s}, \hat{t})}{d\hat{t}} = \frac{\alpha\alpha_s^2}{\hat{s}^4} \left\langle \frac{2}{9} \right\rangle \left\{ 2\text{Re}[F_V(\hat{s})] (\hat{t}^2 + (\hat{s} - 2m_t^2)\hat{t} + \frac{\hat{s}^2}{2} + m_t^4) - 2\text{Re}[F_M(\hat{s})] (\hat{t}^2 + (\hat{s} - 2m_t^2)\hat{t} + m_t^4) \right\}. \quad (3.36)$$

After carrying out the \hat{t} -integration according to Eq. (2.8) the total $q\bar{q} \rightarrow t\bar{t}$ parton cross section to $\mathcal{O}(\alpha\alpha_s^2)$ is given by:

$$\delta\hat{\sigma}_{q\bar{q}}(\hat{s}) = \frac{\alpha\alpha_s^2}{3} \left\langle \frac{2}{9} \right\rangle \frac{1}{\hat{s}^2} \sqrt{1 - \frac{4m_t^2}{\hat{s}}} \left\{ 2\text{Re}[F_V(\hat{s}) + \sum_V F_V^G(\hat{s}, m_q, M_V)] (\hat{s} + 2m_t^2) + \text{Re}[F_M(\hat{s})] (\hat{s} - 4m_t^2) \right\}. \quad (3.37)$$

The quite compact representation of $\delta\mathcal{M}_{gg}$ according to Eq. (3.31) enables its contraction with the gluon fusion Born matrix element Eq. (2.10), which can be parametrised by the help of the standard matrix elements:

$$\mathcal{M}_B^{gg} = 4\pi\alpha_s \left\{ \frac{f_{abc} T_{jl}^c}{\hat{s}} (M_2^{V,t} - 2M_3^{V,t}) + \frac{(-i) T_{jm}^a T_{ml}^b}{\hat{t} - m_t^2} (M_{11}^{V,t} - M_1^{V,t}) + \frac{(-i) T_{jm}^b T_{ml}^a}{\hat{u} - m_t^2} (M_{11}^{V,u} - M_1^{V,u}) \right\} \quad (3.38)$$

and the average (sum) over the degrees of freedom of this process to be done in a pretty handy way. Thus, the $gg \rightarrow t\bar{t}$ parton cross section can be written as follows:

$$\delta \frac{d\hat{\sigma}_{gg}(\hat{s}, \hat{t})}{d\hat{t}} = \frac{\alpha\alpha_s^2}{4\hat{s}^2} \frac{1}{64} 2\text{Re} \left\{ \sum_{j=1,2,3} \left(c^s(j) \frac{1}{\hat{s}} \left[M^t(2, j) F_V(\hat{s}) + M^t(12, j) \frac{(\hat{t} - \hat{u})}{2m_t^2} F_M(\hat{s}) \right] + \sum_{\substack{i=1,\dots,7 \\ 11,\dots,17}} \left(c^t(j) M^t(i, j) \left[\frac{\rho_i^{V,t}(\hat{t}, \hat{s})}{\hat{t} - m_t^2} + \frac{\rho_i^{\Sigma,t}(\hat{t}, \hat{s})}{(\hat{t} - m_t^2)^2} + \rho_i^{\square,t} \right] + c^u(j) M^u(i, j) \left[\frac{\rho_i^{V,u}(\hat{u}, \hat{s})}{\hat{u} - m_t^2} + \frac{\rho_i^{\Sigma,u}(\hat{u}, \hat{s})}{(\hat{u} - m_t^2)^2} + \rho_i^{\square,u} \right] \right) \right) \right\} + \frac{4(M^t(12, 2) + M^t(12, 3))}{(\hat{s} - M_\eta^2)^2 + (M_\eta \Gamma_\eta)^2} \rho_{12}^{\square}(\hat{s}, M_\eta) \quad (3.39)$$

where i numerates the 14 standard matrix elements and $j = 1, 2, 3$ the s, t, u -channel of the Born matrix element. In Eq. (3.39) the following abbreviated forms have been introduced:

- $c^{(s,t,u)}(j)$ denotes the averaged (summed) product of the colour factors of the s, t, u -channel contribution to $\delta\mathcal{M}_{gg}$ and those of the j -th channel of the Born matrix element. The summation (average) over these factors is carried out in App. B.3.
- $M^{(t,u)}(i, j)$ contains the summation over the top quark spins and the average over the gluon polarisation states:

$$M^{(t,u)}(i, j) = \frac{1}{4} \sum_{\lambda} \sum_{s_1, s_2} M_i^{V, (t,u)} \times M_B^{gg, j^*}, \quad (3.40)$$

where $M_B^{gg, j}$ describes the j -th production channel contribution to the Born matrix element:

$$\begin{aligned} M_B^{gg, 1^*} &= \frac{1}{\hat{s}} (M_2^{V, t^*} - 2M_3^{V, t^*}) \\ M_B^{gg, 2^*} &= \frac{1}{\hat{t} - m_t^2} (M_{11}^{V, t^*} - M_1^{V, t^*}) \\ M_B^{gg, 3^*} &= \frac{1}{\hat{u} - m_t^2} (M_{11}^{V, u^*} - M_1^{V, u^*}). \end{aligned} \quad (3.41)$$

A more detailed description how to take the gluon polarisation average has already been given by Eqs. (2.12), (2.13). The explicit expressions for $M^{(t,u)}(i, j)$ can be found in App. B.2.

3.3.1 Discussion

In order to reveal the numerical influence of the electroweak corrections on the top pair production cross section and to investigate their dependence on the free parameters of the MSM, top quark and Higgs boson masses, we introduce a relative correction Δ_i ($i = q\bar{q}, gg$) at the parton level:

$$\hat{\sigma}_i(\hat{s}) = \hat{\sigma}_B^i(\hat{s}) + \delta\hat{\sigma}_i(\hat{s}) = \hat{\sigma}_B^i (1 + \Delta_i). \quad (3.42)$$

In Figs. 9, 10 and Figs. 11, 12 we display our results for the relative correction to the $q\bar{q}$ -annihilation and the gluon fusion subprocesses, respectively, as a function of $\sqrt{\hat{s}}$ for a very low and a very high value of the top quark mass. The increasing influence of the Higgs boson with increasing top quark mass m_t is reflected by the broadening of the area covered by the variation of the Higgs boson mass M_η between 60 and 1000 GeV. Apart from a small region close to the $t\bar{t}$ -production threshold, where the electroweak 1-loop corrections enhance the Born cross section, the relative corrections are negative and increase sizeably with the energy $\sqrt{\hat{s}}$ and the top quark mass. Since the flavour dependence of the $q\bar{q} \rightarrow t\bar{t}$ cross section caused by the initial state electroweak correction is of no numerical significance, $\Delta_{q\bar{q}}$ is representatively shown for a $u\bar{u}$ -pair as initial state. A special feature of the $gg \rightarrow t\bar{t}$ cross section to $\mathcal{O}(\alpha\alpha_s^2)$ is displayed in Figs. 13-16: due to the contribution of the s-channel-Higgs-exchange diagram the relative correction Δ_{gg} contains the characteristic Breit-Wigner resonance structure around $\sqrt{\hat{s}} = M_\eta$.

For the numerical evaluation the electroweak parameters are chosen as follows (taken from the 'Particle Properties Data Booklet', (June 1992)):

$$M_Z = 91.173 \text{ GeV} \quad M_W = 80.22 \text{ GeV} \quad \alpha = \frac{1}{137.035989}.$$

Fig.9: Relative correction to the parton $qq \rightarrow tt$ cross section, $m_t=100$ GeV

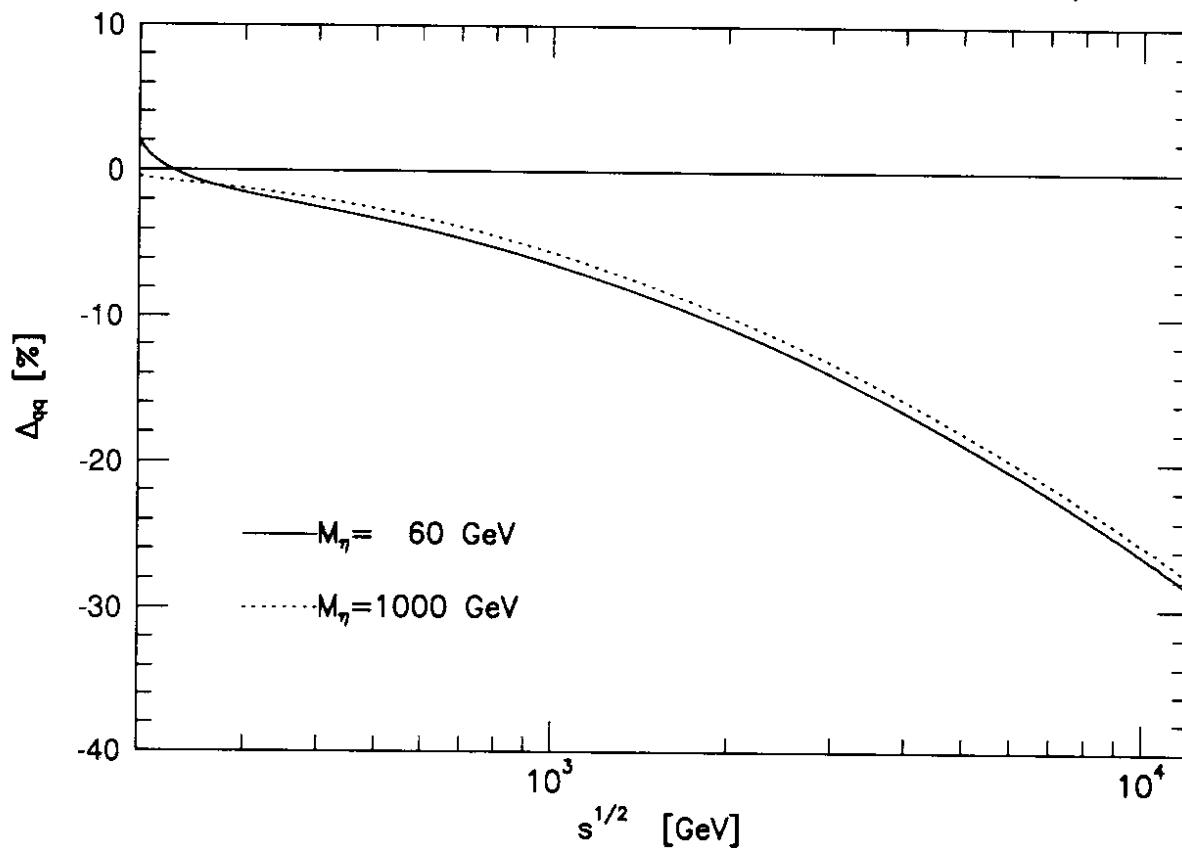


Fig.10: Relative correction to the parton $qq \rightarrow tt$ cross section, $m_t=250$ GeV

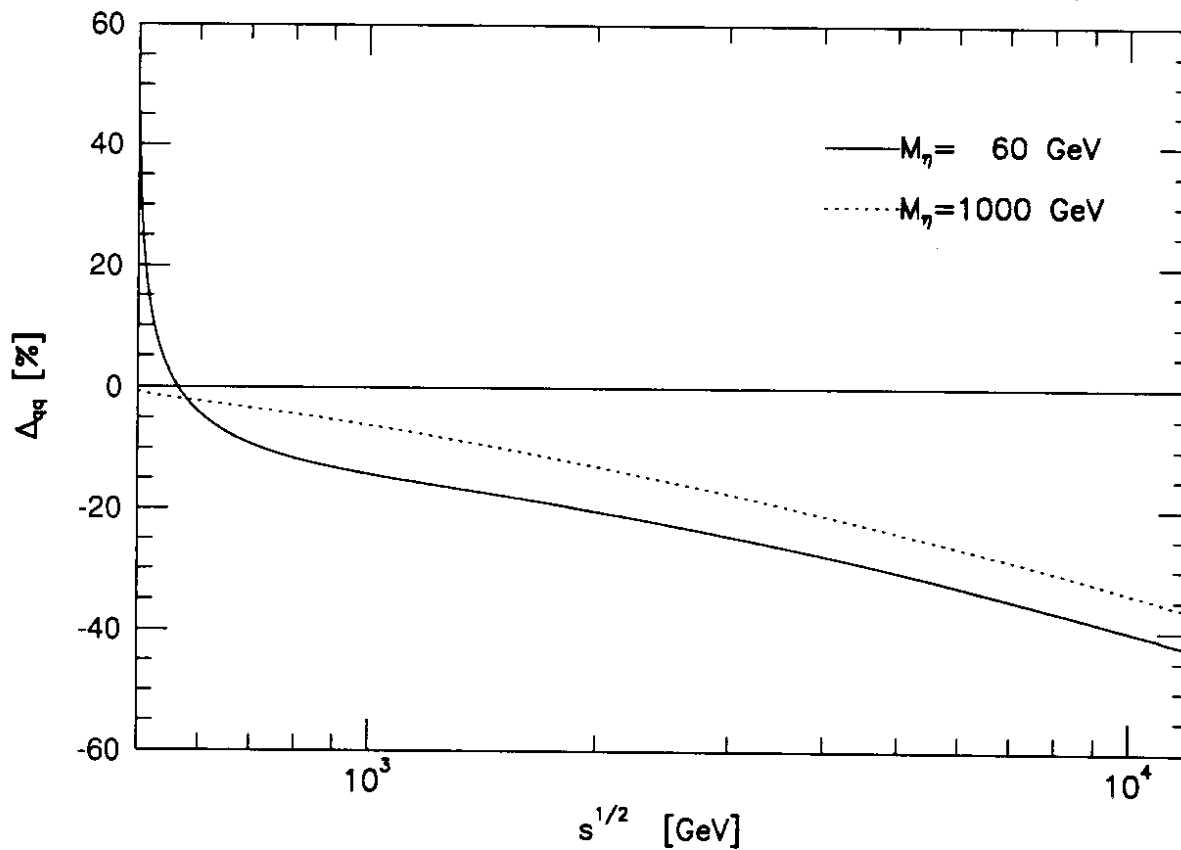


Fig. 11: Relative correction to the parton $gg \rightarrow tt$ cross section, $m_t = 100$ GeV

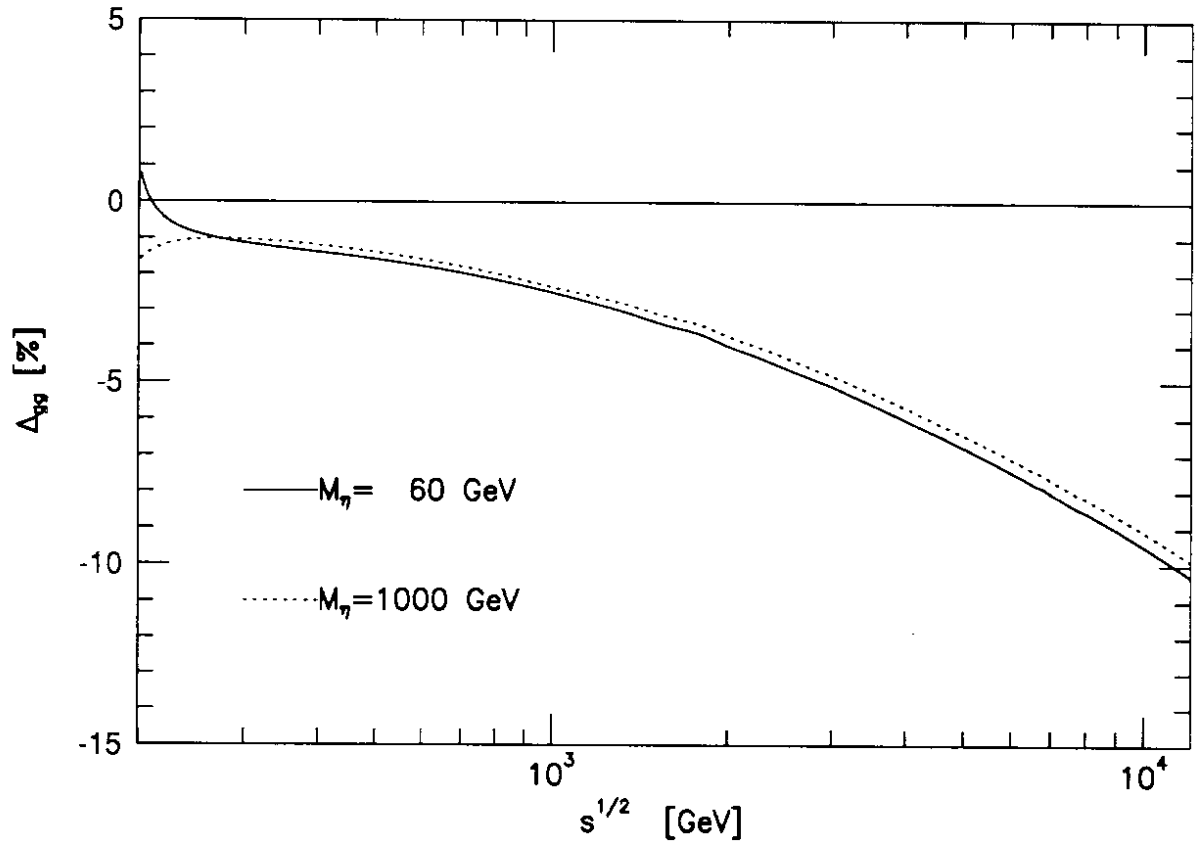
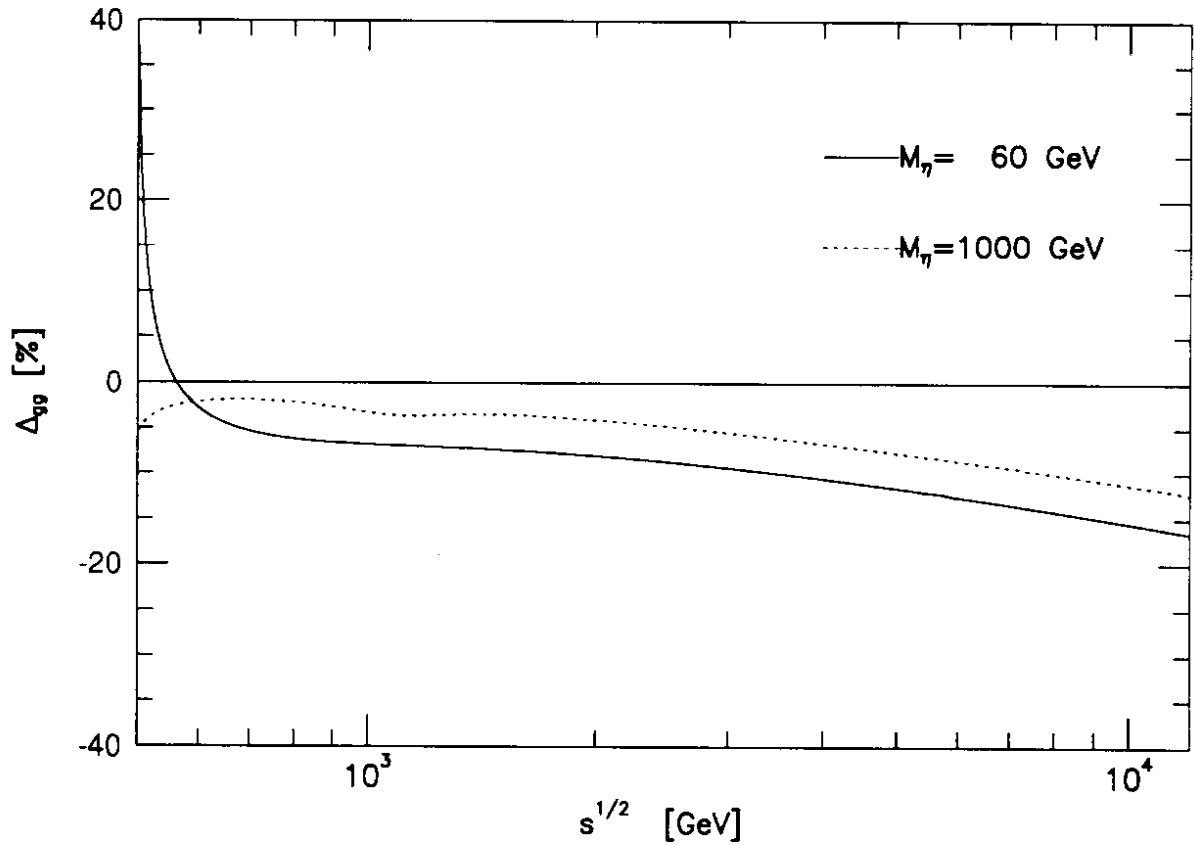


Fig. 12: Relative correction to the parton $gg \rightarrow tt$ cross section, $m_t = 250$ GeV



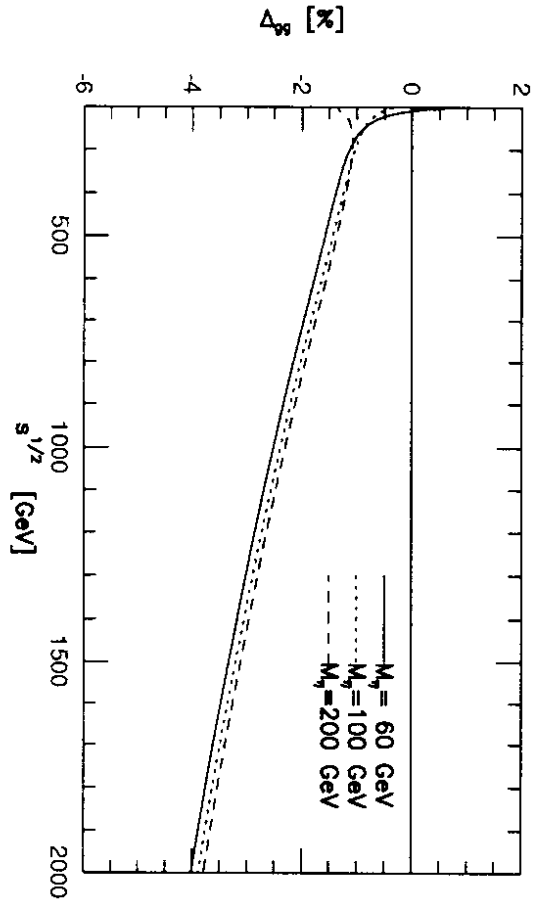


Fig. 13: $m_t=100$ GeV

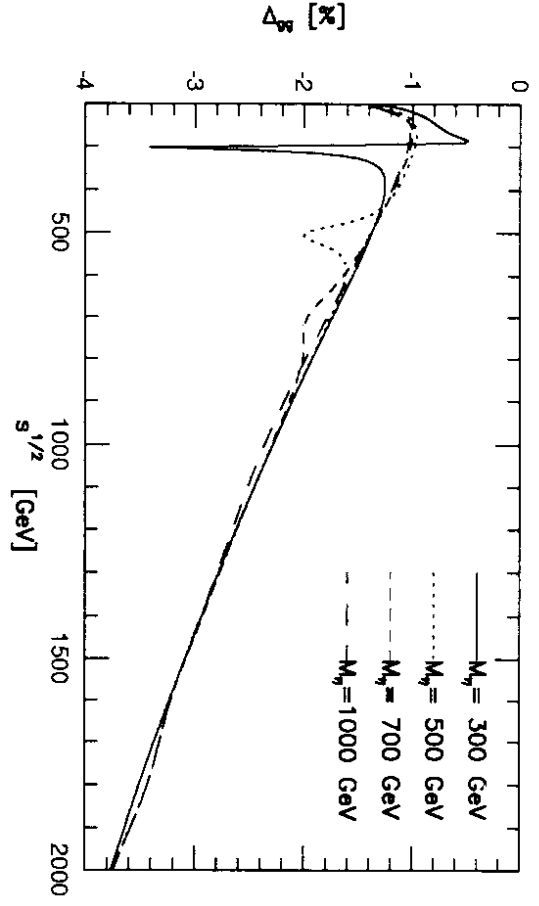


Fig. 14: $m_t=100$ GeV

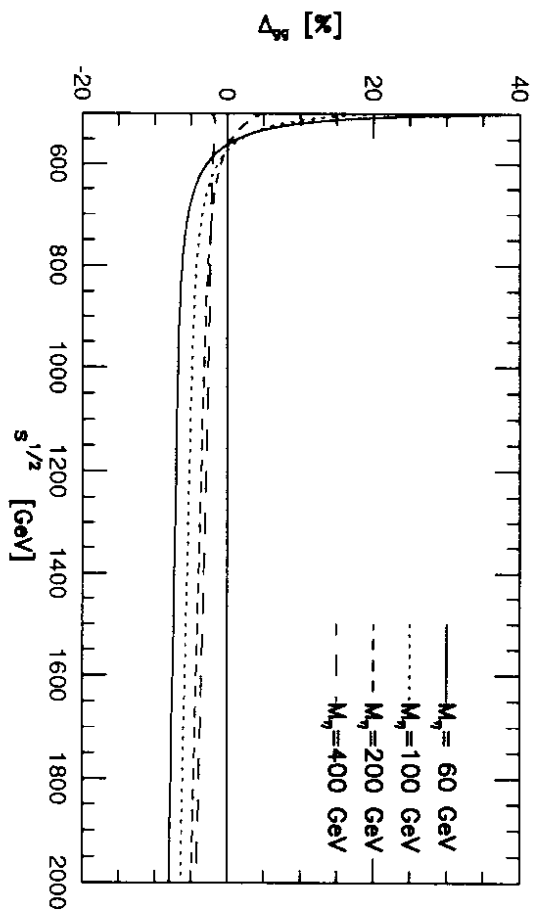


Fig. 15: $m_t=250$ GeV

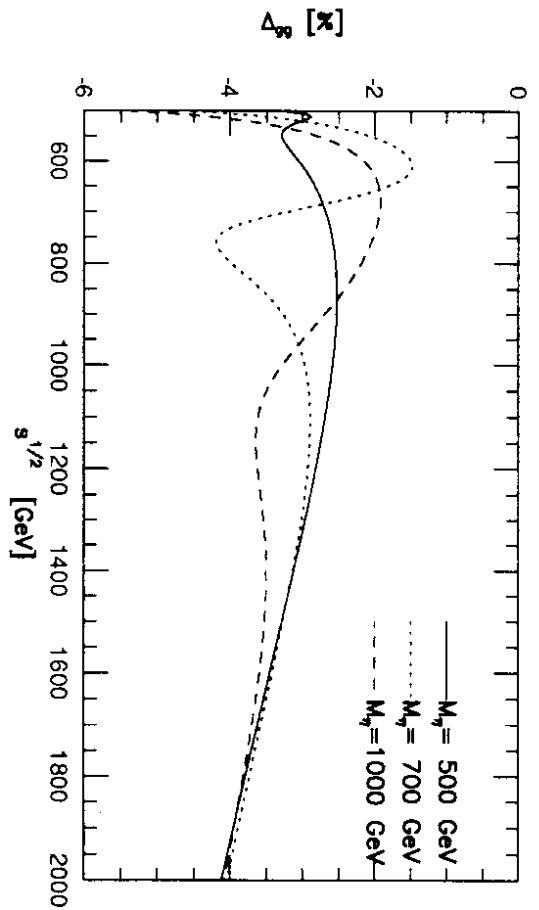


Fig. 16: $m_t=250$ GeV

4 The $pp \rightarrow t\bar{t}X$ -cross section to $\mathcal{O}(\alpha_s^2)$

In the course of the calculation of the leading order hadronic cross section we described the required convolution of the parton cross sections with the parton structure functions according to Eq. (2.20). Using this knowledge and the electroweak next-to-leading order parton cross sections derived in the last section the hadronic total cross section to $\mathcal{O}(\alpha_s^2)$ can be written as follows:

$$\sigma(S) = \int_{\tau_0}^1 \frac{d\tau}{\tau} \left(\frac{1}{S} \frac{dL_{q\bar{q}}}{d\tau} [\hat{s}\hat{\sigma}_{q\bar{q}}] + \frac{1}{S} \frac{dL_{gg}}{d\tau} [\hat{s}\hat{\sigma}_{gg}] \right). \quad (4.1)$$

After the convolution of the parton cross sections according to Eq. (4.1) the observable hadronic cross section $pp \rightarrow t\bar{t}X$ is at high energies mainly determined by the contribution of the convoluted $gg \rightarrow t\bar{t}$ cross section due to the dominance of the gluon distribution. Since the jets from the produced top quarks are better distinguishable from the background at larger scattering angles, it is sensible to impose a cut on the transverse momentum p_t . Analogous to the discussion of the parton cross section in the previous section we define the relative correction Δ :

$$\sigma(S) = \sigma_B(S) + \delta\sigma(S) = \sigma_B(1 + \Delta), \quad (4.2)$$

which reflects the influence of the electroweak 1-loop corrections on the hadronic cross section $\sigma(S)$. Figs. 17, 18 show this relative correction as a function of the Higgs boson mass for two center of mass energies: $\sqrt{S} = 16$ TeV (LHC) and $\sqrt{S} = 32$ TeV (SSC). The next-to-leading order contributions diminish the production cross section compared to the Born result for all Higgs boson masses. The size of Δ is nearly insensitive to the total energy \sqrt{S} . The biggest effect is obtained for small Higgs boson masses; for $M_\eta > 200$ GeV there is very little variation with M_η . The influence of the Higgs sector increases for large top quark masses, as expected from the structure of the Yukawa couplings. For illustration, we have chosen two values for the top quark mass: $m_t = 100$ GeV as an example for a 'light' top quark and $m_t = 250$ GeV for a very heavy top quark. The introduction of a p_t -cut increases the relative correction.

The relatively large corrections up to 40% observed at the parton level are reduced to a few per cent ($\leq 7\%$) for the observable hadronic cross section. This is a consequence of the convolution with the parton densities, which are very small in those regions where the electroweak contributions to the parton processes are large apart from a small region close to the threshold. The positive enhancement of the parton cross section close to the $t\bar{t}$ -threshold for a very light Higgs boson (Fig. 11 and 12) is overcompensated by the negative contributions in the subsequent larger domain, thus yielding an overall negative contribution to $\sigma(S)$.

In summary, the electroweak correction reaches at most -7% for very heavy top quarks and for light Higgs bosons close to the present limit from LEP. In all other cases, they are of the order of a few per cent and thus much smaller than the inherent theoretical uncertainties from QCD.

Fig. 17: Relative correction to the hadronic cross section, $S=(16 \text{ TeV})^2$

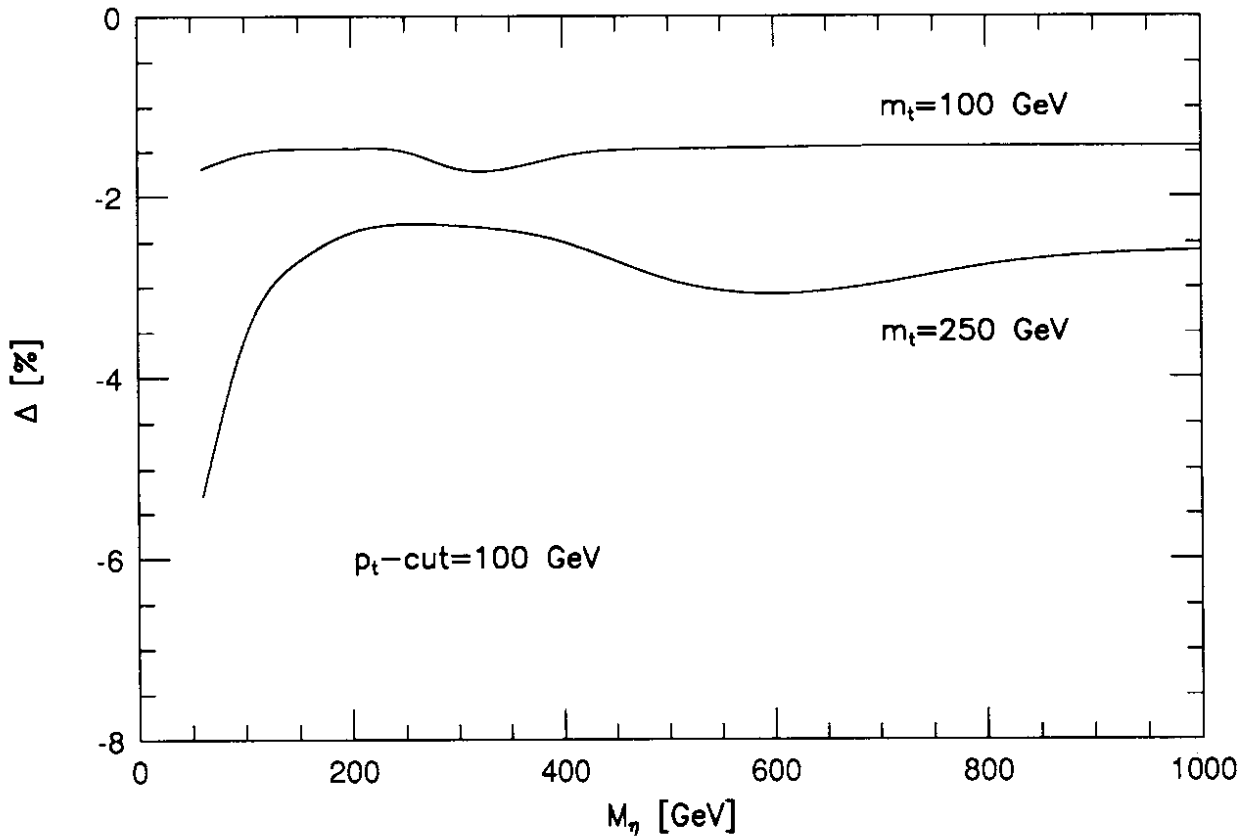
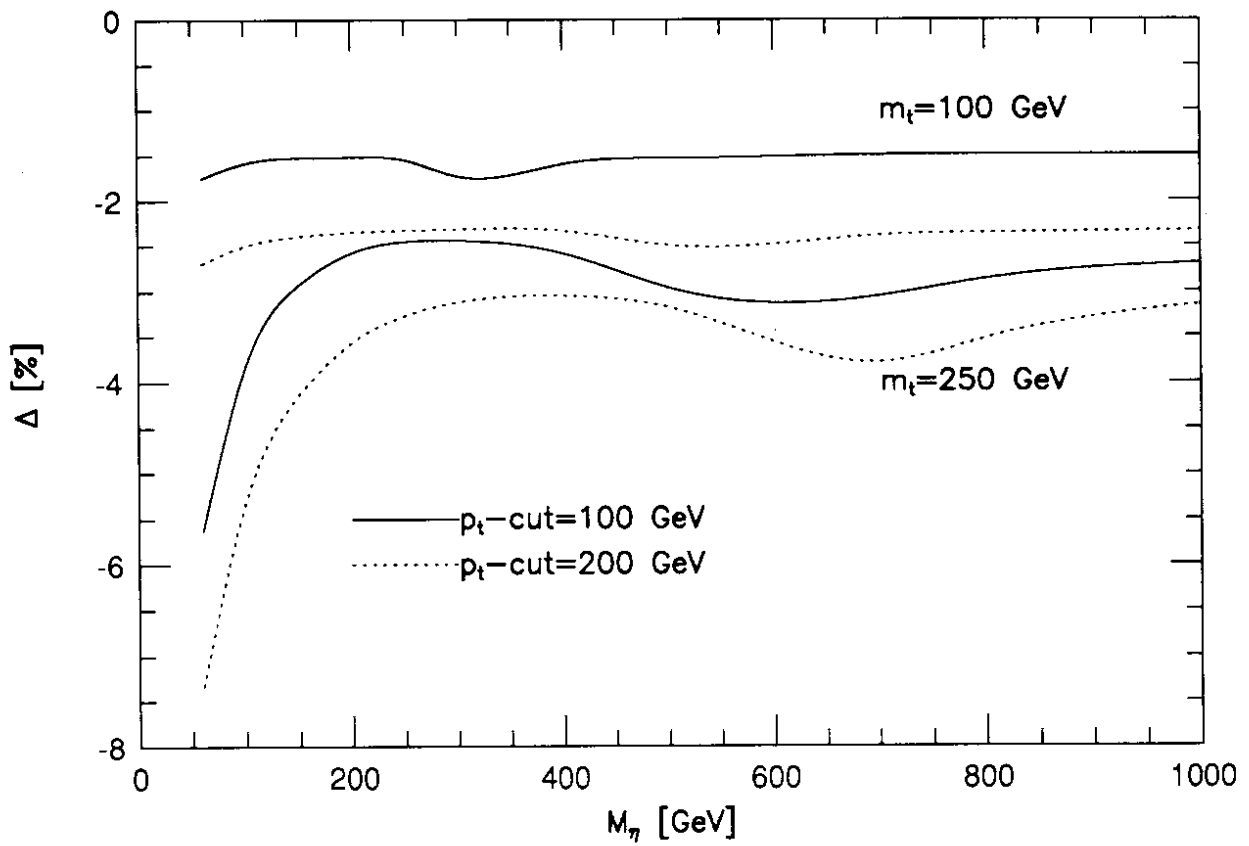


Fig. 18: Relative correction to the hadronic cross section, $S=(32 \text{ TeV})^2$



Appendix A

A.1 Self energies



Figure 9: Feynman diagram for the top quark self energy

The unrenormalised top quark self energy shown in Fig. 9 can be decomposed as follows:

$$\Sigma(\not{p}) = \frac{\alpha}{4\pi} \left[\left(\frac{m_t}{2s_w M_W} \right)^2 \sum_S \Sigma^H(\not{p}) + \sum_V \Sigma^G(\not{p}) \right] \quad (\text{A.1})$$

with

$$\Sigma^{(H,G)}(\not{p}) = \not{p}(\Sigma_V^{(H,G)} - \Sigma_A^{(H,G)} \gamma_5) + m_t \Sigma_S^{(H,G)}, \quad (\text{A.2})$$

where the coefficients of $\Sigma_{V,A,S}^H$ describing the Higgs boson exchange are (m' is the mass of the internal quark):

$$\begin{aligned} \Sigma_V^H(p^2) &= -(c_s^2 + c_p c_p') B_1(p^2, m', M_S) \\ \Sigma_A^H(p^2) &= c_s(c_p + c_p') B_1(p^2, m', M_S) \\ \Sigma_S^H(p^2) &= (c_s^2 - c_p c_p') \frac{m'}{m_t} B_0(p^2, m', M_S) \end{aligned} \quad (\text{A.3})$$

and the gauge boson contribution is given by:

$$\begin{aligned} \Sigma_V^G(p^2) &= -(g_V^2 + g_A^2) [2 B_1(p^2, m', M_V) + 1] \\ \Sigma_A^G(p^2) &= -2g_V g_A [2 B_1(p^2, m', M_V) + 1] \\ \Sigma_S^G(p^2) &= -(g_V^2 - g_A^2) \frac{m'}{m_t} [4 B_0(p^2, m', M_V) - 2]. \end{aligned} \quad (\text{A.4})$$

These scalar functions $\Sigma_{V,S}^{(H,G)}$ yield the renormalisation constants $\delta Z_V^{(H,G)}$ and $\delta m_t^{(H,G)}$, which determine the counter terms required for finite 1-loop corrections due to Higgs boson and massive gauge boson exchange, respectively. According to the Eqs. 3.7, 3.5 they read:

$$\delta Z_V^H(m_t^2) = (c_s^2 + c_p c_p') [B_1(m_t^2, m', M_S) + 2m_t^2 B_1'(m_t^2)] - (c_s^2 - c_p c_p') 2m_t m' B_0'(m_t^2) \quad (\text{A.5})$$

$$\frac{\delta m_t^H}{m_t} = (c_s^2 + c_p c_p') B_1(m_t^2, m', M_S) - (c_s^2 - c_p c_p') \frac{m'}{m_t} B_0(m_t^2, m', M_S) \quad (\text{A.6})$$

$$\delta Z_V^G(m_t^2) = (g_V^2 + g_A^2) [2B_1(m_t^2, m', M_V) + 1 + 4m_t^2 B_1'(m_t^2)] + (g_V^2 - g_A^2) 8m_t m' B_0'(m_t^2) \quad (\text{A.7})$$

$$\frac{\delta m_t^G}{m_t} = (g_V^2 + g_A^2) [2B_1(m_t^2, m', M_V) + 1] + (g_V^2 - g_A^2) \frac{m'}{m_t} [4B_0(m_t^2, m', M_V) - 2] \quad (\text{A.8})$$

The two-point functions $B_{0,1}$ are given in App. C.1 and their derivatives are denoted by $B'_{0,1}(m_t^2) = \frac{\partial B_{0,1}(p^2, m', M_{(s,v)})}{\partial p^2} \Big|_{p^2=m_t^2}$.

A.2 Vectorial and magnetic form factors

The Higgs sector contribution to the s -channel correction in the $q\bar{q}$ -annihilation and the gluon fusion is given in terms of the following form factors:

$$F_V^H(\hat{s}, m_t, M_S) = (c_s^2 + c_p c_p') [-(m_t^2 + m'^2) C_0 + 2C_2^0 - \frac{3}{4} + \hat{s} C_2^- + (4m_t^2 - \hat{s}) C_2^+] \\ - (c_s^2 - c_p c_p') 2m_t m' C_0 + \delta Z_V^H(m_t^2) \quad (\text{A.9})$$

$$F_M^H(\hat{s}, m_t, M_S) = (c_s^2 + c_p c_p') 4m_t^2 [-C_1^+ + 2C_2^+] - (c_s^2 - c_p c_p') 4m_t m' C_1^+ . \quad (\text{A.10})$$

Analogously, the gauge boson contribution is given by:

$$F_V^G(\hat{s}, m_q, M_V) = (g_V^2 + g_A^2) 2 [(3m_q^2 - m'^2 - \hat{s}) C_0 - \frac{5}{4} + 2C_2^0 - 2(4m_q^2 - \hat{s}) C_1^+ \\ + (4m_q^2 - \hat{s}) C_2^+ + \hat{s} C_2^-] + \delta Z_V^G(m_q^2) \quad (\text{A.11})$$

$$F_M^G(\hat{s}, m_q, M_V) = (g_V^2 + g_A^2) 8m_q^2 [C_0 - 3C_1^+ + 2C_2^+] \\ - (g_V^2 - g_A^2) 8m_q m' [C_0 - 2C_1^+] , \quad (\text{A.12})$$

where $m_q = m_t$ has to be taken in case of the final state contribution and $m_q = m_u, m_d, \dots$ for the initial state of the $q\bar{q}$ -annihilation subprocess. The explicit expressions for the functions $[C_0, C_1^+, C_2^{0-+}](\hat{s}, m', m', M_{S,V})$ are given in [12].

A.3 Coefficients of the standard matrix elements

The t -channel electroweak next-to-leading order gluon fusion matrix element is given in terms of the following coefficients of the standard matrix elements $M_i^{V,t}$ (only non-zero terms and coefficients of $M_i^{V,t}$, which contribute even after the interference with the Born matrix element, will be given explicitly):

- the vertex correction:

$$H_1^{V,t} = 2(c_s^2 + c_p c_p') [B_0(0, m', m') - 2C_2^0 - (m_t^2 + m'^2 - M_S^2) C_0 + (\hat{t} - m_t^2) C_1^2] \\ - 4(c_s^2 - c_p c_p') m_t m' C_0 + 2\delta Z_V^H(m_t^2) \\ H_4^{V,t} = (-2)(c_s^2 + c_p c_p') (\hat{t} - m_t^2) [C_1^2 + C_2^2 + C_2^{12}] \\ H_{11}^{V,t} = 2(c_s^2 + c_p c_p') [2C_2^0 - B_0(0, m', m') + (\hat{t} + m'^2 - M_S^2) C_0 + (\hat{t} - m_t^2) C_1^1] \\ + 2(c_s^2 - c_p c_p') \frac{m'}{m_t} (\hat{t} + m_t^2) C_0 - 2\delta Z_V^H(m_t^2) \\ H_{14}^{V,t} = 2(c_s^2 + c_p c_p') [C_1^1 + C_1^2 + C_2^1 + C_2^2 + 2C_2^{12}] \\ + 2(c_s^2 - c_p c_p') \frac{m'}{m_t} [C_1^1 + C_1^2] \\ H_{16}^{V,t} = -4 H_{14}^{V,t} \quad (\text{A.13})$$

and

$$G_1^{V,t} = 4(g_V^2 + g_A^2) [(2m_t^2 - m'^2 + M_V^2 + \hat{t}) C_0 - 2C_2^0 + B_0(0, m', m') - \frac{1}{2}$$

$$\begin{aligned}
& + (3m_t^2 + \hat{t}) C_1^1 + 2(\hat{t} + m_t^2) C_1^2] + 2 \delta Z_V^G(m_t^2) \\
G_4^{V,t} &= (-4) (g_V^2 + g_A^2) (\hat{t} - m_t^2) [C_0 + C_1^1 + 2C_1^2 + C_2^2 + C_2^{12}] \\
G_{11}^{V,t} &= 4 (g_V^2 + g_A^2) [-(2\hat{t} - m'^2 + m_t^2 - M_V^2) C_0 + 2C_2^0 - B_0(0, m', m') + \frac{1}{2} \\
& \quad - 2(\hat{t} + m_t^2) C_1^1 - (3\hat{t} + m_t^2) C_1^2] - 2 \delta Z_V^G(m_t^2) \\
G_{14}^{V,t} &= 4 (g_V^2 + g_A^2) [2C_0 + 3C_1^1 + 3C_1^2 + C_2^1 + C_2^2 + 2C_2^{12}] \\
& \quad - 8 (g_V^2 - g_A^2) \frac{m'}{m_t} [C_0 + C_1^1 + C_1^2] \\
G_{16}^{V,t} &= -4 G_{14}^{V,t}, \tag{A.14}
\end{aligned}$$

where the C -functions $C_i^j(\hat{t}, m', m', M_{S,V})$ are expressed in terms of two-point functions and the scalar three-point function $C_0(\hat{t}, m', m', M_{S,V})$ as it is described in App. C.2.

- the t -channel self energy contribution:

$$\begin{aligned}
(H, G)_1^{\Sigma,t} &= -[(\hat{t} + m_t^2) \hat{\Sigma}_V^{t,(H,G)}(\hat{t}) + 2 m_t^2 \hat{\Sigma}_S^{t,(H,G)}(\hat{t})] \\
(H, G)_{11}^{\Sigma,t} &= 2 \hat{t} \hat{\Sigma}_V^{t,(H,G)}(\hat{t}) + (\hat{t} + m_t^2) \hat{\Sigma}_S^{t,(H,G)}(\hat{t}), \tag{A.15}
\end{aligned}$$

where $\hat{\Sigma}_{V,S}^{t,(H,G)}$ denote the coefficients of the finite \hat{t} -channel top quark self energy according to the decomposition of Eqs. A.1, A.2 (with $\not{p} = \not{p}_3 - \not{p}_1$):

$$\begin{aligned}
\hat{\Sigma}_V^{t,H}(\hat{t}) &= -(c_s^2 + c_p c_p') B_1(\hat{t}, m', M_S) + \delta Z_V^H(m_t^2) \\
\hat{\Sigma}_S^{t,H}(\hat{t}) &= (c_s^2 - c_p c_p') \frac{m'}{m_t} B_0(\hat{t}, m', M_S) + \frac{\delta m_t^H}{m_t} - \delta Z_V^H(m_t^2) \tag{A.16}
\end{aligned}$$

and

$$\begin{aligned}
\hat{\Sigma}_V^{t,G}(\hat{t}) &= 2 (g_V^2 + g_A^2) [-B_1(\hat{t}, m', M_V) - \frac{1}{2}] + \delta Z_V^G(m_t^2) \\
\hat{\Sigma}_S^{t,G}(\hat{t}) &= (g_V^2 - g_A^2) 4 \frac{m'}{m_t} [-B_0(\hat{t}, m', M_V) + \frac{1}{2}] + \frac{\delta m_t^G}{m_t} - \delta Z_V^G(m_t^2). \tag{A.17}
\end{aligned}$$

- the box diagram contribution:

$$\begin{aligned}
H_1^{\square,t} &= (c_s^2 + c_p c_p') [C_0 + (M_S^2 - m_t^2 - m'^2) D_0 + (m'^2 - m_t^2) D_1^2 - 6D_2^0 \\
& \quad - \hat{t} (2D_2^2 + D_3^2) - 2(\hat{t} + m_t^2) (D_2^{12} + D_3^{21}) \\
& \quad - 6D_3^{02} - 2m_t^2 D_3^{12} + (\hat{s} - 2m_t^2) D_3^{123}] \\
& \quad + (c_s^2 - c_p c_p') [-2m' m_t D_0] \\
H_2^{\square,t} &= (c_s^2 + c_p c_p') [-2D_2^0 - 2D_3^{02}] \\
H_4^{\square,t} &= 2(c_s^2 + c_p c_p') [(m_t^2 - m'^2) (D_1^1 + D_1^2) + 2D_2^0 + m_t^2 (2D_2^1 + 2D_2^{13} + D_3^1) \\
& \quad + (\hat{t} + m_t^2) D_2^2 + (\hat{t} + 5m_t^2) D_2^{12} + 2(D_3^{01} + 2D_3^{02}) \\
& \quad + \hat{t} D_3^2 + (\hat{t} + 3m_t^2) D_3^{12} + (3\hat{t} + 2m_t^2) D_3^{21} \\
& \quad + (3m_t^2 - \hat{s}) D_3^{13} + (\hat{t} - \hat{s} + 3m_t^2) D_3^{123}] \\
H_6^{\square,t} &= 2(c_s^2 + c_p c_p') [D_2^2 + 2D_2^{12} + D_3^2 + 2D_3^{13} + 4D_3^{21} + 2D_3^{123}]
\end{aligned}$$

$$\begin{aligned}
H_{11}^{\square,t} &= (-2)(c_s^2 + c_p c_p') [C_0 + (M_S^2 - m'^2) D_0 + (\hat{t} + 2m_t^2 - m'^2) D_1^1 \\
&\quad + (\hat{t} + m_t^2) (D_2^1 + D_2^{13} + D_3^{12} + D_3^{123}) \\
&\quad + \hat{t} (D_1^2 + 2D_2^{12} + D_3^{21}) + 2D_2^0 \\
&\quad + 6D_3^{01} + m_t^2 D_3^1 - (\hat{s} - 3m_t^2) D_3^{13}] \\
&\quad + (c_s^2 - c_p c_p') \frac{m'}{m_t} [(m'^2 + m_t^2 - M_S^2) D_0 - 2(\hat{t} + m_t^2) D_1^1 - 2\hat{t} D_1^2 - C_0] \\
H_{12}^{\square,t} &= 4(c_s^2 + c_p c_p') [D_2^0 + 2D_3^{01} + D_3^{02}] + 4(c_s^2 - c_p c_p') \frac{m'}{m_t} D_2^0 \\
H_{14}^{\square,t} &= 2(c_s^2 + c_p c_p') [2D_1^1 + D_1^2 + 2D_2^1 + D_2^2 + 4D_2^{12} + 2D_2^{13}] \\
&\quad + 2(c_s^2 - c_p c_p') \frac{m'}{m_t} [2D_1^1 + D_1^2] \\
H_{16}^{\square,t} &= (-4)(c_s^2 + c_p c_p') [4D_1^1 + 2D_1^2 + 3D_2^2 + 12D_2^{12} + 2D_3^1 + D_3^2 \\
&\quad + 6(D_2^1 + D_2^{13} + D_3^{12} + D_3^{13} + D_3^{21} + D_3^{123})] \\
&\quad - 4(c_s^2 - c_p c_p') \frac{m'}{m_t} [4D_1^1 + 2D_1^2 + 2D_2^1 + D_2^2 + 4D_2^{12} + 2D_2^{13}] \tag{A.18}
\end{aligned}$$

and

$$\begin{aligned}
G_1^{\square,t} &= 2(g_V^2 + g_A^2) [-C_0 + (5m_t^2 + m'^2 - \hat{s} - M_V^2) D_0 - 2(\hat{s} - 4m_t^2) D_1^1 \\
&\quad - (\hat{s} + m'^2 - 5m_t^2) D_1^2 + 6D_2^0 + \hat{t}(2D_2^2 + D_3^2) \\
&\quad + 2(\hat{t} + m_t^2) (D_2^{12} + D_3^{21}) + 6D_3^{02} + 2m_t^2 D_3^{12} - (\hat{s} - 2m_t^2) D_3^{123}] \\
&\quad + (g_V^2 - g_A^2) [-8m' m_t D_0] \\
G_2^{\square,t} &= 2(g_V^2 + g_A^2) [-C_0 + (m_t^2 + m'^2 - M_V^2) D_0 - (m'^2 - m_t^2) D_1^2 \\
&\quad + 4D_2^0 + \hat{t}(2D_2^2 + D_3^2) + 2(\hat{t} + m_t^2) (D_2^{12} + D_3^{21}) \\
&\quad + 4D_3^{02} + 2m_t^2 D_3^{12} - (\hat{s} - 2m_t^2) D_3^{123}] \\
&\quad + (g_V^2 - g_A^2) [-4m' m_t D_0] \\
G_4^{\square,t} &= 4(g_V^2 + g_A^2) [C_0 + (M_V^2 + m_t^2 - m'^2) D_0 + (5m_t^2 - m'^2 - \hat{s}) D_1^1 \\
&\quad + (\hat{t} + m_t^2) (D_1^2 + D_3^{12} + D_3^{123}) - 4D_2^0 \\
&\quad + (\hat{t} + m_t^2 - \hat{s}) D_2^{12} - (\hat{s} - 2m_t^2) (D_2^1 + D_2^{13}) \\
&\quad + 2(D_3^{01} - D_3^{02}) + m_t^2 D_3^1 + \hat{t} D_3^{21} + (3m_t^2 - \hat{s}) D_3^{13}] \\
G_6^{\square,t} &= 4(g_V^2 + g_A^2) [2D_1^2 + 6D_2^{12} + 3D_2^2 + D_3^2 + 2D_3^{12} + 4D_3^{21} + 2D_3^{123}] \\
G_{11}^{\square,t} &= 4(g_V^2 + g_A^2) [C_0 - (m_t^2 + m'^2 + \hat{t} - M_V^2) D_0 - (\hat{t} + m'^2) D_1^1 \\
&\quad + (\hat{t} + m_t^2) (D_2^1 + D_2^{13} + D_3^{12} + D_3^{123}) + \hat{t} (2D_2^{12} + D_3^{21}) \\
&\quad - 2D_2^0 + 6D_3^{01} + m_t^2 (D_3^1 - D_1^2) - (\hat{s} - 3m_t^2) D_3^{13}] \\
&\quad + (g_V^2 - g_A^2) 2 \frac{m'}{m_t} (\hat{s} + 2m_t^2 + 2\hat{t}) D_0 \\
G_{12}^{\square,t} &= (-4)(g_V^2 + g_A^2) [(M_V^2 + m_t^2 - m'^2) D_0 + C_0 + 2(\hat{t} + 2m_t^2 - m'^2) D_1^1 + \\
&\quad + (2\hat{t} + m_t^2 - m'^2) D_1^2 + 2(\hat{t} + m_t^2) (D_2^1 + D_2^{13}) + 2(3\hat{t} + m_t^2) D_2^{12} \\
&\quad + \hat{t} (2D_2^2 + D_3^2) + 8D_3^{01} + 4D_3^{02} + 2m_t^2 D_3^1 + 2(\hat{t} + 2m_t^2) D_3^{12} \\
&\quad + 2(2\hat{t} + m_t^2) D_3^{21} + 2(3m_t^2 - \hat{s}) D_3^{13} + (4m_t^2 - \hat{s} + 2\hat{t}) D_3^{123}]
\end{aligned}$$

$$\begin{aligned}
& +(g_V^2 - g_A^2) 4 \frac{m'}{m_t} [(M_V^2 + m_t^2 - m'^2) D_0 + 2(\hat{t} + m_t^2) D_1^1 + 2\hat{t} D_1^2 + C_0 - 4D_2^0] \\
G_{14}^{\square,t} &= 4(g_V^2 + g_A^2) [2D_0 + 2D_1^1 + D_1^2 - D_2^1 - D_2^2 - 4D_2^{12} - 2D_2^{13}] \\
& +(g_V^2 - g_A^2) [-8 \frac{m'}{m_t} D_0] \\
G_{16}^{\square,t} &= (-8) (g_V^2 + g_A^2) [4D_0 + 12D_1^1 + 6D_1^2 + 6D_2^1 + 3D_2^2 + 12D_2^{12} + 6D_2^{13} \\
& + 2D_3^1 + 6D_3^{12} + 6D_3^{13} + D_3^2 + 6D_3^{21} + 6D_3^{123}] \\
& + 16(g_V^2 - g_A^2) \frac{m'}{m_t} [2D_0 + 4D_1^1 + 2D_1^2 + 2D_2^1 + D_2^2 + 4D_2^{12} + 2D_2^{13}], \quad (\text{A.19})
\end{aligned}$$

where the three- and four-point functions are denoted by $C_0 = C_0(\hat{s}, m', m', m')$ and $[D_0, D_i^j] = [D_0, D_i^j](\hat{t}, m', m', m', M_{S,V})$, respectively. The decomposition of the four-point integrals is given in App. C.3.

- and the s -channel-Higgs-exchange diagram ($\tau = \frac{4m_t^2}{\hat{s}}$) [13]:

$$H_{12}^{\square}(\hat{s}, M_\eta) = c_s^2 [\hat{s} - M_\eta^2 - i M_\eta \Gamma_\eta] 4 [1 - (1 - \tau) \frac{\hat{s}}{2} C_0(\hat{s}, m_t, m_t, m_t)] \quad (\text{A.20})$$

with

$$\frac{\hat{s}}{2} C_0(\hat{s}, m_t, m_t, m_t) = \frac{1}{4} [\log \frac{1 + \sqrt{1 - \tau}}{1 - \sqrt{1 - \tau}} - i\pi]^2. \quad (\text{A.21})$$

The standard model Higgs boson decay width Γ_η in lowest order perturbation theory is given in [14].

Appendix B

B.1 The standard matrix elements

The t -channel standard matrix elements of the gluon fusion are given by:

$$\begin{aligned}
M_1^{\{V,A\},t} &= \bar{u}(p_2) \not{\epsilon}_4 (\not{p}_1 - \not{p}_3) \not{\epsilon}_3 \{1, \gamma_5\} v(p_1) \\
M_2^{\{V,A\},t} &= \bar{u}(p_2) (\not{p}_4 - \not{p}_3) \{1, \gamma_5\} v(p_1) \epsilon_4 \epsilon_3 \\
M_3^{\{V,A\},t} &= \bar{u}(p_2) (\not{\epsilon}_4 \epsilon_3 p_4 - \not{\epsilon}_3 \epsilon_4 p_3) \{1, \gamma_5\} v(p_1) \\
M_4^{\{V,A\},t} &= \bar{u}(p_2) (\not{\epsilon}_4 \epsilon_3 p_1 - \not{\epsilon}_3 \epsilon_4 p_2) \{1, \gamma_5\} v(p_1) \\
M_5^{\{V,A\},t} &= \bar{u}(p_2) (\not{p}_4 - \not{p}_3) \{1, \gamma_5\} v(p_1) \epsilon_4 p_3 \epsilon_3 p_4 \\
M_6^{\{V,A\},t} &= \bar{u}(p_2) (\not{p}_4 - \not{p}_3) \{1, \gamma_5\} v(p_1) \epsilon_4 p_2 \epsilon_3 p_1 \\
M_7^{\{V,A\},t} &= \bar{u}(p_2) (\not{p}_4 - \not{p}_3) \{1, \gamma_5\} v(p_1) (\epsilon_4 p_3 \epsilon_3 p_1 + \epsilon_4 p_2 \epsilon_3 p_4) \quad (\text{B.1})
\end{aligned}$$

$$\begin{aligned}
M_{11}^{\{V,A\},t} &= \bar{u}(p_2) \not{\epsilon}_4 \not{\epsilon}_3 \{1, \gamma_5\} v(p_1) m_t \\
M_{12}^{\{V,A\},t} &= \bar{u}(p_2) \{1, \gamma_5\} v(p_1) \epsilon_4 \epsilon_3 m_t \\
M_{13}^{\{V,A\},t} &= \bar{u}(p_2) (\not{\epsilon}_4 \not{p}_4 \epsilon_3 p_4 \pm \not{p}_3 \not{\epsilon}_3 \epsilon_4 p_3) \{1, \gamma_5\} v(p_1) m_t
\end{aligned}$$

$$\begin{aligned}
M_{14}^{\{V,A\},t} &= \bar{u}(p_2) (\not{\epsilon}_4 \not{p}_4 \epsilon_3 p_1 \pm \not{p}_3 \not{\epsilon}_3 \epsilon_4 p_2) \{1, \gamma_5\} v(p_1) m_t \\
M_{15}^{\{V,A\},t} &= \bar{u}(p_2) \{1, \gamma_5\} v(p_1) \epsilon_4 p_3 \epsilon_3 p_4 m_t \\
M_{16}^{\{V,A\},t} &= \bar{u}(p_2) \{1, \gamma_5\} v(p_1) \epsilon_4 p_2 \epsilon_3 p_1 m_t \\
M_{17}^{\{V,A\},t} &= \bar{u}(p_2) \{1, \gamma_5\} v(p_1) (\epsilon_4 p_3 \epsilon_3 p_1 \pm \epsilon_4 p_2 \epsilon_3 p_4) m_t
\end{aligned} \tag{B.2}$$

The u -channel standard matrix elements $M_i^{\{V,A\},u}$ follow from $M_i^{\{V,A\},t}$ by the substitutions:

$$p_3 \leftrightarrow p_4 \text{ and } \epsilon_3 \leftrightarrow \epsilon_4 .$$

B.2 Interference with the Born matrix element

The $gg \rightarrow t\bar{t}$ cross section to $\mathcal{O}(\alpha_s^2)$ is given in terms of the factors $M^{(t,u)}(i, j)$ ($i = 1, \dots, 17$, $j = 1, 2, 3$), which describe the required interference of the electroweak next-to-leading order matrix element with the Born matrix element according to Eq. (3.40). For the gauge choice according to Eqs. (2.12), (2.13) these factors have been obtained as follows:

$$\begin{aligned}
M^t(1, 1) &= -4 [m_t^2 - \hat{t}]^2 [m_t^2 - \hat{u}] / \hat{s}^2 \\
M^t(1, 2) &= 2 [8m_t^6 \hat{t} - 7m_t^4 \hat{t}^2 + 2m_t^2 \hat{t}^3 + 4m_t^6 \hat{u} - 20m_t^4 \hat{t} \hat{u} + 12m_t^2 \hat{t}^2 \hat{u} \\
&\quad - 3\hat{t}^3 \hat{u} - m_t^4 \hat{u}^2 + 6m_t^2 \hat{t} \hat{u}^2 - \hat{t} \hat{u}^3] / [\hat{s}^2 (\hat{t} - m_t^2)] \\
M^t(1, 3) &= 2 [m_t^4 - \hat{t} \hat{u}] [4m_t^4 - 2m_t^2 (\hat{t} + \hat{u}) + (\hat{u} - \hat{t})^2] / [\hat{s}^2 (\hat{u} - m_t^2)]
\end{aligned} \tag{B.3}$$

$$\begin{aligned}
M^t(2, 1) &= 4 [m_t^2 - \hat{t}] [m_t^2 - \hat{u}] / \hat{s} \\
M^t(2, 2) &= [4m_t^6 - 4m_t^4 \hat{t} + 2m_t^2 \hat{t}^2 - 8m_t^4 \hat{u} + 8m_t^2 \hat{t} \hat{u} - 4\hat{t}^2 \hat{u} + 2m_t^2 \hat{u}^2] / [\hat{s} (\hat{t} - m_t^2)] \\
M^t(2, 3) &= [4m_t^6 - 2m_t^2 \hat{s}^2 - 12m_t^4 \hat{u} + 4m_t^2 \hat{s} \hat{u} \\
&\quad + 12m_t^2 \hat{u}^2 - 4\hat{s} \hat{u}^2 - 4\hat{u}^3] / [\hat{s} (\hat{u} - m_t^2)]
\end{aligned} \tag{B.4}$$

$$\begin{aligned}
M^t(4, 1) &= 2 [\hat{u} - \hat{t}] [m_t^2 - \hat{t} \hat{u}] / \hat{s}^2 \\
M^t(4, 2) &= 2 [m_t^4 - \hat{t} \hat{u}] [4m_t^4 - 4\hat{u} \hat{t} + \hat{s} \hat{u} + 2\hat{s}^2 - m_t^2 \hat{s}] / [\hat{s}^2 (\hat{t} - m_t^2)] \\
M^t(4, 3) &= 2 [m_t^4 - \hat{t} \hat{u}] [10m_t^4 - 5m_t^2 \hat{t} - 7m_t^2 \hat{u} \\
&\quad + \hat{t}^2 + 2\hat{u}^2 - \hat{u} \hat{t}] / [\hat{s}^2 (\hat{u} - m_t^2)]
\end{aligned} \tag{B.5}$$

$$\begin{aligned}
M^t(6, 1) &= -2 [m_t^2 - \hat{t}] [m_t^2 - \hat{u}] [m_t^4 - \hat{u} \hat{t}] / \hat{s}^2 \\
M^t(6, 2) &= [-2m_t^{10} + m_t^8 \hat{t} - m_t^6 \hat{t}^2 + 5m_t^8 \hat{u} - 2m_t^6 \hat{t} \hat{u} + 2m_t^4 \hat{t}^2 \hat{u} \\
&\quad + m_t^2 \hat{t}^3 \hat{u} - m_t^6 \hat{u}^2 - 6m_t^4 \hat{t} \hat{u}^2 \\
&\quad + 4m_t^2 \hat{t}^2 \hat{u}^2 - 3\hat{t}^3 \hat{u}^2 + m_t^2 \hat{t} \hat{u}^3 + \hat{t}^2 \hat{u}^3] / [\hat{s}^2 (\hat{t} - m_t^2)] \\
M^t(6, 3) &= [2m_t^{10} - 5m_t^8 \hat{t} + m_t^6 \hat{t}^2 - m_t^8 \hat{u} + 2m_t^6 \hat{t} \hat{u} + 6m_t^4 \hat{t}^2 \hat{u} \\
&\quad - m_t^2 \hat{t}^3 \hat{u} + m_t^6 \hat{u}^2 - 2m_t^4 \hat{t} \hat{u}^2 \\
&\quad - 4m_t^2 \hat{t}^2 \hat{u}^2 - \hat{t}^3 \hat{u}^2 - m_t^2 \hat{t} \hat{u}^3 + 3\hat{t}^2 \hat{u}^3] / [\hat{s}^2 (\hat{u} - m_t^2)]
\end{aligned} \tag{B.6}$$

$$\begin{aligned}
M^t(11, 1) &= 2 m_t^2 [\hat{t} - \hat{u}] / \hat{s} \\
M^t(11, 2) &= 2 m_t^2 [-2m_t^4 - 2m_t^2 \hat{s} + \hat{s}^2 + 4m_t^2 \hat{t} - 2\hat{t}^2] / [\hat{s} (\hat{t} - m_t^2)] \\
M^t(11, 3) &= 4 m_t^2 [-m_t^4 + \hat{t} \hat{u}] / [\hat{s} (\hat{u} - m_t^2)]
\end{aligned} \tag{B.7}$$

$$\begin{aligned}
M^t(12, 1) &= 2 m_t^2 [\hat{t} - \hat{u}] / \hat{s} \\
M^t(12, 2) &= m_t^2 [-4m_t^4 + 2m_t^2 \hat{s} - \hat{s}^2 + 8m_t^2 \hat{u} - 6 \hat{s} \hat{u} - 4 \hat{u}^2] / [\hat{s} (\hat{t} - m_t^2)] \\
M^t(12, 3) &= m_t^2 [-4m_t^4 - 2m_t^2 \hat{s} + \hat{s}^2 + 8m_t^2 \hat{u} - 2 \hat{s} \hat{u} - 4 \hat{u}^2] / [\hat{s} (\hat{u} - m_t^2)] \quad (\text{B.8})
\end{aligned}$$

$$\begin{aligned}
M^t(14, 1) &= 0 \\
M^t(14, 2) &= 2 m_t^2 [\hat{u} \hat{t} - m_t^4] / (\hat{t} - m_t^2) \\
M^t(14, 3) &= 2 m_t^2 [\hat{u} \hat{t} - m_t^4] / (\hat{u} - m_t^2) \quad (\text{B.9})
\end{aligned}$$

$$\begin{aligned}
M^t(16, 1) &= m_t^2 [\hat{u} - \hat{t}] [m_t^4 - \hat{u} \hat{t}] / \hat{s}^2 \\
M^t(16, 2) &= m_t^2 [m_t^4 - \hat{t} \hat{u}] [8m_t^4 - 2m_t^2 \hat{t} + \hat{t}^2 + 2m_t^2 \hat{u} - 8 \hat{t} \hat{u} - \hat{u}^2] / [2 \hat{s}^2 (\hat{t} - m_t^2)] \\
M^t(16, 3) &= m_t^2 [m_t^4 - \hat{t} \hat{u}] [8m_t^4 + 2m_t^2 \hat{s} - \hat{s}^2 - 16m_t^2 \hat{u} \\
&\quad + 6 \hat{s} \hat{u} + 8 \hat{u}^2] / [2 \hat{s}^2 (\hat{u} - m_t^2)]. \quad (\text{B.10})
\end{aligned}$$

Since $M^t(i, j) = 0$ for $i = 3, 5, 7, 13, 15, 17$, the coefficients of the concerned standard matrix elements do not contribute.

The interference of the u -channel contribution to the gluon fusion matrix element with the Born matrix element leads to the factors $M^u(i, j)$ according to Eq. 3.40. They are derived from $M^t(i, j)$ by using the following substitutions:

$$\begin{aligned}
M^u(i, 1) &= -M^t(i, 1)(\hat{t} \rightarrow \hat{u}) \\
M^u(i, 2) &= M^t(i, 3)(\hat{t} \rightarrow \hat{u}) \\
M^u(i, 3) &= M^t(i, 2)(\hat{t} \rightarrow \hat{u}). \quad (\text{B.11})
\end{aligned}$$

B.3 The colour factors

The summation (average) over the colour degrees of freedom in the course of the derivation of the parton cross sections leads to the following colour factors:

$$\begin{aligned}
c^s(1) &= \sum_{\substack{a,b,c; \\ j,l}} (f_{abc} T_{jl}^c) (T_{jl}^d f_{abd})^* = 3 \sum_{c,d} \delta_{cd} \text{Tr}\{T^c T^d\} = 12 \\
c^t(1) &= \sum_{\substack{a,b,c; \\ j,l}} (iT_{jm}^a T_{ml}^b) (T_{jl}^c f_{abc})^* = -c^s(2) = -6 \\
c^u(1) &= \sum_{\substack{a,b,c; \\ j,l}} (iT_{jm}^b T_{ml}^a) (T_{jl}^c f_{abc})^* = -c^s(3) = 6 \\
c^t(2) &= \sum_{\substack{a,b,c; \\ j,l}} (iT_{jm}^a T_{ml}^b) (-iT_{jm}^a T_{ml}^b)^* = c^u(3) = -\frac{16}{3} \\
c^u(2) &= \sum_{\substack{a,b,c; \\ j,l}} (iT_{jm}^b T_{ml}^a) (-iT_{jm}^a T_{ml}^b)^* = c^t(3) = \frac{2}{3}. \quad (\text{B.12})
\end{aligned}$$

Appendix C

C.1 The two-point integrals

The dimensional regularisation enables the extraction of the UV-divergency in the scalar and vectorial two-point integrals $B_{0,1}$:

$$\frac{i}{16\pi^2}(B_0; p_\mu B_1)(p^2, m', M) = \mu^{4-D} \int \frac{d^D k}{(2\pi)^D} \frac{(1; k_\mu)}{[k^2 - m'^2][(k+p)^2 - M^2]}, \quad (\text{C.1})$$

so that they can be written as follows [12]:

$$B_0(p^2, m', M) = \Delta - \int_0^1 dx \log \frac{x^2 p^2 - x(p^2 + m'^2 - M^2) + m'^2 - i\epsilon}{\mu^2} \quad (\text{C.2})$$

$$B_1(p^2, m', M) = \frac{1}{2p^2} [m'^2(\Delta - \log \frac{m'^2}{\mu^2} + 1) - M^2(\Delta - \log \frac{M^2}{\mu^2} + 1) + (M^2 - m'^2 - p^2) B_0(p^2, m', M)]. \quad (\text{C.3})$$

The divergency is conventionally expressed by $\Delta = \frac{2}{4-D} - \gamma_E + \log 4\pi$ with γ_E being the Euler constant.

C.2 The three-point integrals

In the course of the calculation of the vertex correction $\Lambda_\mu^{(t1,t2)}$ to the gluon-top-vertex in the t -channel of the gluon fusion the following D-dimensional three-point integrals occurred:

$$\frac{i}{16\pi^2}(C_0; C_\mu; C_{\mu\nu}) = \mu^{4-D} \int \frac{d^D k}{(2\pi)^D} \frac{(1; k_\mu; k_\mu k_\nu)}{\Delta_1 \Delta_2 \Delta_3} \quad (\text{C.4})$$

with

$$\Delta_1 = k^2 - M^2, \quad \Delta_2 = (k - p_2)^2 - m'^2, \quad \Delta_3 = (k + p_1 - p_3)^2 - m'^2.$$

For its derivation a decomposition according to [15] has been used ($C_i^j = C_i^j(\hat{t}, m', m', M)$):

$$C_\mu = -p_{2\mu} C_1^1 + (p_1 - p_3)_\mu C_1^2 \quad (\text{C.5})$$

$$C_{\mu\nu} = p_{2\mu} p_{2\nu} C_2^1 + (p_1 - p_3)_\mu (p_1 - p_3)_\nu C_2^2 + g_{\mu\nu} C_2^0 - (p_{2\mu} (p_1 - p_3)_\nu + (p_1 - p_3)_\mu p_{2\nu}) C_2^{12} \quad (\text{C.6})$$

with the coefficients ($B_0(0) = B_0(0, m', m')$):

$$(\hat{t} - m_t^2)^2 C_1^1 = (\hat{t} + m_t^2) B_0(m_t^2, M, m') - 2\hat{t} B_0(\hat{t}, M, m') + (\hat{t} - m_t^2) [(M^2 - m'^2 - \hat{t}) C_0 + B_0(0)] \quad (\text{C.7})$$

$$(\hat{t} - m_t^2)^2 C_1^2 = (\hat{t} + m_t^2) B_0(\hat{t}, M, m') - 2m_t^2 B_0(m_t^2, M, m') + (\hat{t} - m_t^2) [(m'^2 - M^2 + m_t^2) C_0 - B_0(0)] \quad (\text{C.8})$$

$$(\text{C.9})$$

$$2C_2^0 = M^2 C_0 + \frac{1}{2}[(M^2 + m_t^2 - m'^2) C_1^1 + (M^2 + \hat{t} - m'^2) C_1^2 + 1 + B_0(0)] \quad (\text{C.10})$$

$$(\hat{t} - m_t^2)^2 C_2^1 = 4\hat{t} C_2^0 + (\hat{t} + m_t^2) B_1(m_t^2, M, m') + (\hat{t} - m_t^2) [(M^2 - m'^2 - \hat{t}) C_1^1 - \frac{1}{2} B_0(0)] \quad (\text{C.11})$$

$$(\hat{t} - m_t^2)^2 C_2^2 = 4m_t^2 C_2^0 + \frac{1}{\hat{t} + m_t^2} \left\{ (\hat{t} - m_t^2)^2 [B_1(\hat{t}, M, m') + \frac{1}{2} B_0(0)] + (m'^2 - m_t^2 - M^2) C_1^2 + 2m_t^2 [2m_t^2 B_1(m_t^2, M, m') + (\hat{t} - m_t^2) [(M^2 - m_t^2 - m'^2) C_1^1 - \frac{1}{2} B_0(0)]] \right\} \quad (\text{C.12})$$

$$(\hat{t} - m_t^2)^2 C_2^{12} = -2m_t^2 B_1(m_t^2, M, m') - 2(\hat{t} + m_t^2) C_2^0 - (\hat{t} - m_t^2) [(M^2 - m_t^2 - m'^2) C_1^1 - \frac{1}{2} B_0(0)]. \quad (\text{C.13})$$

C.3 The four-point integrals

The calculation of the box diagram contribution requires the derivation of the four-point integrals given by $(\Delta_4 = (k + p_1)^2 - m'^2)$:

$$\frac{i}{16\pi^2} (D_0; D_\mu; D_{\mu\nu}; D_{\mu\nu\rho}) = \int \frac{d^4 k}{(2\pi)^4} \frac{(1; k_\mu; k_\mu k_\nu; k_\mu k_\nu k_\rho)}{\Delta_1 \Delta_2 \Delta_3 \Delta_4}. \quad (\text{C.14})$$

According to [15] the vectorial and tensorial four-point integrals have been reduced by the following decompositions:

$$D_\mu = -p_{2\mu} D_1^1 + (p_1 - p_3)_\mu D_1^2 + p_{1\mu} D_1^3 \quad (\text{C.15})$$

$$D_{\mu\nu} = p_{2\mu} p_{2\nu} D_2^1 + (p_1 - p_3)_\mu (p_1 - p_3)_\nu D_2^2 + p_{1\mu} p_{1\nu} D_2^3 + g_{\mu\nu} D_2^0 - (p_{2\mu} (p_1 - p_3)_\nu + (p_1 - p_3)_\mu p_{2\nu}) D_2^{12} - (p_{2\mu} p_{1\nu} + p_{1\mu} p_{2\nu}) D_2^{13} + ((p_1 - p_3)_\mu p_{1\nu} + p_{1\mu} (p_1 - p_3)_\nu) D_2^{23} \quad (\text{C.16})$$

$$D_{\mu\nu\rho} = -p_{2\mu} p_{2\nu} p_{2\rho} D_3^1 + (p_1 - p_3)_\mu (p_1 - p_3)_\nu (p_1 - p_3)_\rho D_3^2 + p_{1\mu} p_{1\nu} p_{1\rho} D_3^3 - (g_{\mu\nu} p_{2\rho} + \text{cycl.}) D_3^{01} + (g_{\mu\nu} (p_1 - p_3)_\rho + \text{cycl.}) D_3^{02} + (g_{\mu\nu} p_{1\rho} + \text{cycl.}) D_3^{03} + ((p_1 - p_3)_\mu p_{2\nu} p_{2\rho} + \text{cycl.}) D_3^{12} - (p_{2\mu} (p_1 - p_3)_\nu (p_1 - p_3)_\rho + \text{cycl.}) D_3^{21} + (p_{1\mu} p_{2\nu} p_{2\rho} + \text{cycl.}) D_3^{13} - (p_{2\mu} p_{1\nu} p_{1\rho} + \text{cycl.}) D_3^{31} + (p_{1\mu} (p_1 - p_3)_\nu (p_1 - p_3)_\rho + \text{cycl.}) D_3^{23} + ((p_1 - p_3)_\mu p_{1\nu} p_{1\rho} + \text{cycl.}) D_3^{32} - (p_{2\mu} (p_1 - p_3)_\nu p_{1\rho} + \text{perm.}) D_3^{123}, \quad (\text{C.17})$$

where *cycl.* and *perm.* denote cyclic commutation and permutation of the indices, respectively. The contraction of the four-point integrals with the tensors built up of the external momenta leads to a linear equation system for the coefficients D_i^j . Its solution is explicitly described in [15].

References

- [1] D0 COLLABORATION, talk presented by S.Protopopescu at the XXVIIIth Rencontre de Moriond: Electroweak Interactions and Unified Theories, Les Arcs 1993
CDF COLLABORATION, talk presented by B.Harral at the XXVIIIth Rencontre de Moriond: Electroweak Interactions and Unified Theories, Les Arcs 1993
- [2] G.ROLANDI, CERN-PPE/92-175 (1992), to appear in: Proceedings of the XXVI International Conference on High Energy Physics, Dallas 1992
- [3] M.GLÜCK, J.F.OWENS, E.REYA, *Phys. Rev.* **D17** (1978), 2324
B.L.COMBRIDGE, *Nucl. Phys.* **B151** (1978), 429
J.BABCOCK, D.SILVERS, S.WOLFRAM, *Phys. Rev.* **D18** (1978), 162
K.HAGIWARA, T.YOSHINO, *Phys. Lett.* **80B** (1979), 282
L.M.JONES, H.WYLD, *Phys. Rev* **D17** (1978), 782
H.GEORGI ET AL., *Ann. Phys.(N.Y.)* **114** (1978), 273
- [4] U.BAUR, A.D.MARTIN, *Phys. Lett.* **232B** (1989), 519
- [5] P.NASON, S.DAWSON, R.K.ELLIS, *Nucl. Phys.* **B303** (1988), 607
G.ALTARELLI, M.DIEMOZ, G.MARTINELLI, P.NASON, *Nucl. Phys.* **B308** (1988), 724
W.BEENAKKER, H.KUIJF, W.L.VAN NEERVEN, J.SMITH, *Phys. Rev.* **D40** (1989), 54
- [6] V.FADIN, V.KHOZE, *JETP Lett.* **46** (1987), 525
V.FADIN, V.KHOZE, T.SJÖSTRAND, *Z. Phys.* **C48** (1990), 613
- [7] W.BEENAKKER, W.HOLLIK, *Phys. Lett.* **269B** (1991), 425
W.BEENAKKER, W.HOLLIK, S.VAN DER MARCK, *Nucl. Phys.* **B365** (1991), 24
R.J.GUTH, J.H.KÜHN, *Nucl. Phys.* **B368** (1992), 38
A.DENNER, R.J.GUTH, J.H.KÜHN, *Nucl. Phys.* **B377** (1992), 3
- [8] R.K.ELLIS ET AL., *Nucl. Phys.* **B152** (1979), 285
- [9] R.K.ELLIS, W.J.STIRLING, in 'Precision Tests of the Standard Model at High Energy Colliders', Proceedings of XVIII International Meeting on Fundamental Physics and XXI G.I.F.T. International Seminar on Theoretical Physics, Santander 1990, eds. F. del Águila, A. Méndez, A.Ruiz, World Scientific, Singapore 1991
- [10] P.N.HARRIMAN, A.D.MARTIN, W.J.STIRLING, R.G.ROBERTS, Rutherford Appleton Laboratory Preprint RAL-90-007, Jan. 1990
- [11] G.PASSARINO, M.VELTMAN, *Nucl. Phys.* **B160** (1979), 151
- [12] W.HOLLIK, *Fortschr. Phys.* **38** (1990) 3, 165
- [13] Z.KUNSZT, W.J.STIRLING, in Proceedings of Large Hadron Collider Workshop Vol. II, CERN 90-10, eds. G.Jarlskog, D.Rein, Aachen 1990
- [14] J.F.GUNION, H.E.HABER, G.KANE, S.DAWSON, 'The Higgs Hunter's Guide', Addison-Wesley 1990
- [15] T.SACK, Ph.D. thesis, Julius-Maximilian-Universität Würzburg 1987